

**INSTITUTO POTOSINO DE INVESTIGACIÓN  
CIENTÍFICA Y TECNOLÓGICA, A.C.**

**POSGRADO EN CIENCIAS EN BIOLOGIA MOLECULAR**

**NEURONAL RECEPTORS INVOLVED IN THE  
INFLAMMATORY PROCESS**

Tesis que presenta

**Telma Liliana Ramos Lomas**

Para obtener el grado de

**Doctora en Ciencias en Biología Molecular**

**CoDirectores de la Tesis:**

**Dr. Carlos Barajas López**

**Dr. Stephen Vanner**

San Luis Potosí, S.L.P., Julio, 2012



**INSTITUTO POTOSINO DE INVESTIGACIÓN  
CIENTÍFICA Y TECNOLÓGICA, A.C.**

**POSGRADO EN CIENCIAS EN BIOLOGIA MOLECULAR**

**NEURONAL RECEPTORS INVOLVED IN THE  
INFLAMMATORY PROCESS**

Tesis que presenta

**Telma Liliana Ramos Lomas**

Para obtener el grado de

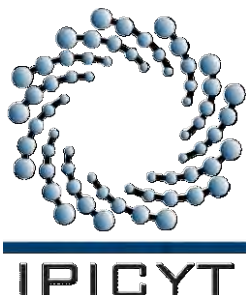
**Doctora en Ciencias en Biología Molecular**

**CoDirectores de la Tesis:**

**Dr. Carlos Barajas López**

**Dr. Stephen Vanner**

San Luis Potosí, S.L.P., Julio, 2012



## CONSTANCIA DE APROBACIÓN DE LA TESIS

La tesis "**Neuronal Receptors Involved in the Inflammatory Process**" presentada para obtener el grado de Doctora en Ciencias en Biología Molecular fue elaborada por **Telma Liliana Ramos Lomas** y aprobada el **15 de Julio, 2012** por los suscritos, designados por el Colegio de Profesores de la División de Biología Molecular del Instituto Potosino de Investigación Científica y Tecnológica, A.C.

---

Dr. Carlos Barajas López  
(CoDirector de Tesis)

---

Dr. Stephen Vanner  
(CoDirector de Tesis)

---

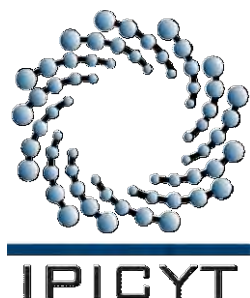
Dr. Rubén H. López Revilla  
(Asesor de Tesis)

---

Dra. Marcela Miranda Morales  
(Asesor de Tesis)

---

Dr. Luis M. Montaña Ramírez  
(Asesor de Tesis)



## **CRÉDITOS INSTITUCIONALES**

Esta tesis fue elaborada en el Laboratorio de Neurobiología de la División de Biología Molecular del Instituto Potosino de Investigación Científica y Tecnológica A.C. y en la Unidad de Investigación de Enfermedades Intestinales (GIDRU) de la Universidad de Queen, bajo la codirección de los doctores Carlos Barajas López y Stephen Vanner.

Durante la realización del trabajo el autor recibió una beca académica del Consejo Nacional de Ciencia y Tecnología (174914) y del Instituto Potosino de Investigación Científica y Tecnológica, A. C.



# Instituto Potosino de Investigación Científica y Tecnológica, A.C.

## Acta de Examen de Grado

El Secretario Académico del Instituto Potosino de Investigación Científica y Tecnológica, A.C., certifica que en el Acta 048 del Libro Primero de Actas de Exámenes de Grado del Programa de Doctorado en Ciencias en Biología Molecular está asentado lo siguiente:

En la ciudad de San Luis Potosí a los 24 días del mes de agosto del año 2012, se reunió a las 16:00 horas en las instalaciones del Instituto Potosino de Investigación Científica y Tecnológica, A.C., el Jurado integrado por:

<b>Dr. Rubén Hipólito López Revilla</b>	<b>Presidente</b>	<b>IPICYT</b>
<b>Dr. Luis Manuel Montañó Ramírez</b>	<b>Secretario</b>	<b>UNAM</b>
<b>Dr. Carlos Barajas López</b>	<b>Sinodal</b>	<b>IPICYT</b>
<b>Dr. Sergio Zarazúa Guzmán</b>	<b>Sinodal externo</b>	<b>UASLP</b>

a fin de efectuar el examen, que para obtener el Grado de:

**DOCTORA EN CIENCIAS EN BIOLOGÍA MOLECULAR**

sustentó la C.

**Telma Liliana Ramos Lomas**

sobre la Tesis intitulada:

*Neuronal receptors involved in the inflammatory process*

que se desarrolló bajo la dirección de


**Dr. Carlos Barajas López**

El Jurado, después de deliberar, determinó

**APROBARLA**

Dándose por terminado el acto a las 18:30 horas, procediendo a la firma del Acta los integrantes del Jurado. Dando fe el Secretario Académico del Instituto.

A petición de la interesada y para los fines que a la misma convengan, se extiende el presente documento en la ciudad de San Luis Potosí, S.L.P., México, a los 24 días del mes de agosto de 2012.

  
**Dr. Marcial Bonilla Marín**  
Secretario Académico

  
**Mtra. Ivonne Lizette Cuevas Vélez**  
Jefa del Departamento del Posgrado



## DEDICATORIAS

A mis padres...

porque por ustedes un millón de imposibles han sido posibles.

A mis hermanos...

porque han sido todo en vida, cómplices y soplones,  
fuerza y debilidad, aliento y burla... y siguen dándome tanto,  
que estaré en deuda siempre.

A mis sobrinos...

porque son la esperanza...no solo mía, del mundo entero,  
esperamos que sean mejores de lo nunca fuimos.

## AGRADECIMIENTOS

Al IPICYT por todos los recursos invertidos en mi formación académica.

Al CONACYT por la beca otorgada (TLRL 174914).

A mis codirectores de tesis, el Dr. Carlos Barajas López por todas las oportunidades que me ha brindado para desarrollar mi potencial, y por los conocimientos y consejos compartidos siempre de forma generosa, *and to Dr. Stephen Vanner for the opportunity he gave me to become part of his staff and for his patience... Thanks.*

A la Dra. Marcela Miranda Morales, porque siempre estuvo ahí para brindar un consejo oportuno, por el tiempo que dedico a la revisión de esta tesis y porque en muchos momentos evitó que me volviera un poco loca.

Al Dr. Rubén López Revilla porque siempre me ha dado excelentes sugerencias de cómo expresarme y mejorar el trabajo que realizo, si este escrito es mejor que mis tesis anteriores ha sido gracias a lo que aprendí en sus cursos.

Al Dr. Luis M. Montaña Ramírez por formar parte de mi comité tutorial, por el tiempo que dedicó a la revisión de este escrito.

Al Dr. Sergio Zarazúa Guzmán, por aceptar ser parte del jurado de mi examen y por los consejos que me ofreció desinteresadamente.

A la Lic. Rosa Espinosa Luna (Rosi para los que la queremos), primero por su invaluable apoyo y enseñanzas en varias técnicas de laboratorio y manejo de equipo, porque siempre procuró que nunca faltara material para desarrollar esta investigación; y segundo, por su amistad incondicional, por escucharme y apoyarme cuando más lo he necesitado, valoraré siempre todo de lo que se desprendió para ofrecérmelo desinteresadamente... ¡Gracias Rosi!.

A mis compañeros y amigos de generación, porque aunque lejos, cuando los vuelvo a ver me sigo sintiendo conectada a ustedes como antes.

A los miembros del laboratorio de neurobiología por sus críticas que señalaron los fallos que hicieron mejorar mis presentaciones.

A mi familia, porque simplemente, sin ustedes no estaría aquí, esto no sería posible y no habría razón para haberlo realizado, siempre he pensado que lo más simple es lo más valioso, es más...No tiene precio.

## CONTENT

<b>CONSTANCIA DE APROBACIÓN DE LA TESIS .....</b>	<b>II</b>
<b>CREDITOS INSTITUCIONALES .....</b>	<b>III</b>
<b>ACTA DE EXAMEN .....</b>	<b>IV</b>
<b>DEDICACION .....</b>	<b>V</b>
<b>AGRADECIMIENTOS.....</b>	<b>VI</b>
<b>CONTENT .....</b>	<b>VII</b>
<b>LIST OF FIGURES AND TABLES.....</b>	<b>IX</b>
<b>ABBREVIATIONS .....</b>	<b>XI</b>
<b>GLOSSARY .....</b>	<b>XII</b>
<b>ABSTRACT .....</b>	<b>XIII</b>
<b>RESUMEN.....</b>	<b>XIV</b>
<b>I. GENERAL BACKGROUND .....</b>	<b>1</b>
INFLAMMATORY BOWEL DISEASE.....	1
IRRITABLE BOWEL SYNDROME.....	2
INTESTINAL DISEASES AND PAIN .....	4
NOCICEPTIVE PATHWAY .....	6
PAIN AND INFLAMMATION .....	9
TOLL LIKE RECEPTOR (TLR).....	11
TOLL-LIKE RECEPTOR 4 (TLR4).....	13
PATHWAY OF SIGNALING .....	14
DIRECT BACKGROUND.....	17
THE RATIONALE BEHIND THIS STUDY.....	18
<b>II. HYPOTHESIS.....</b>	<b>19</b>
<b>III. GENERAL AIM.....</b>	<b>19</b>
SPECIFIC OBJETIVES .....	19
<b>IV. MATERIAL AND METHODS.....</b>	<b>20</b>
ANIMALS AND CELL CULTURES.....	20
SEMIQUANTITATIVE RT-PCR .....	22
WESTERN BLOTTING .....	24
FAST BLUE INJECTION .....	25
IMMUNOHISTOCHEMISTRY .....	25
ELISA METHOD TO QUANTIFY TNF- $\alpha$ INDUCED BY LPS IN CULTURE SUPERNATANTS	26
ANTIBODIES AND REAGENTS .....	27
ACUTE APPLICATION EXPERIMENTS .....	27
LPS EFFECTS ON COLONIC AFFERENT NERVES .....	29
CHRONIC DSS INFLAMMATORY MODEL.....	30
<b>V. RESULTS.....</b>	<b>32</b>



A. DRG NEURONS THAT PROYECT TO THE COLON SHOW THE TRANSCRIPT OF PATTERN RECOGNITION RECEPTORS. ....	32
B. DRG NEURONS PROJECTING TO THE COLON SHOW IMMUNOREACTIVITY FOR TOLL-LIKE RECEPTOR 4 .....	32
C. LPS ACTIVATES NF-κB PATHWAY .....	33
D. INCREASE EXPRESSION OF CITOKINES .....	37
E. LPS INCREASE CITOKINE RELEASE.....	37
F. COLONIC AFFERENT RESPONSES TO LPS .....	39
<b>VI. DISCUSSION.....</b>	<b>41</b>
<b>VII. CONCLUSION.....</b>	<b>50</b>
<b>VIII. APPENDIX A.....</b>	<b>51</b>
CLONACIÓN DE RECEPTORES IONOTROPICOS INVOLUCRADOS EN EL PROCESO INFLAMATORIO. ....	51
ANTECEDENTES .....	51
MATERIALES Y MÉTODOS .....	54
<i>Secuencia genómica y del cDNA de los receptores P2X5 y 5HT3A.....</i>	<i>54</i>
<i>Clonación del receptor P2X5 y 5HT3A.....</i>	<i>54</i>
RESULTADOS .....	56
<i>P2X5 de intestino de ratón.....</i>	<i>56</i>
<i>P2X5 de intestino de cobayo.....</i>	<i>57</i>
<i>5HT3A de intestino de cobayo.....</i>	<i>61</i>
DISCUSIÓN Y CONCLUSIONES. ....	64
<b>IX. REFERENCES .....</b>	<b>65</b>
<b>X. APPENDIX B.....</b>	<b>72</b>

## LIST OF FIGURES AND TABLES

<b>Figure 1.</b> Different nociceptive neurons detect different modalities of pain. ....	7
<b>Figure 2.</b> Scheme of the nociception pathway. ....	8
<b>Figure 3.</b> Graphical representation of the hyperalgesia and allodynia concepts.....	9
<b>Figure 4.</b> Structure of the Toll Like Receptors (TLRs) includes a leucine-rich repeat (LRR) and a Toll/IL-1R (TIR) domain. ....	11
<b>Figure 5.</b> Toll-like Receptors (TLRs) ligand specificities. ....	12
<b>Figure 6.</b> Schematic representation of lipopolysaccharides (LPS) trafficking .....	13
<b>Figure 7.</b> Schematic representation of NF- $\kappa$ B proteins family. ....	15
<b>Figure 8.</b> Schematic diagram of LPS trafficking and TLR4-mediated inflammatory signaling in the mammalian host. ....	16
<b>Figure 9.</b> Photographs of the dorsal root ganglia (DRGs) corresponding to the T9-T13 spinal segments. ....	21
<b>Figure 10.</b> Chart Flow of Experimental Protocols.....	22
<b>Figure 11.</b> Setup to record the multiunitary activity and the intestinal distension..	31
<b>Figure 12.</b> Toll-like receptors (TLRs) and supplementary proteins are express in dorsal root ganglia (DRG) neurons that project to the colon .....	33
<b>Figure 13.</b> Colonic Projecting DRG Neuron showing fluorecence for the retrograde marker Fast Blue. ....	34
<b>Figure 14.</b> Slides of mouse DRG show Immunoreactivity for TLR4. ....	35
<b>Figure 15.</b> NF $\kappa$ B Pathway is activated by LPS.....	36
<b>Figure 16.</b> LPS and ultrapure LPS increased the expression of cytokines in DRG neurons.....	38
<b>Figure 17.</b> LPS increase release of TNF $\alpha$ .....	39
<b>Figure 18.</b> Effects of standard-grade LPS on excitability are not mediated by TLR4. ....	40
<b>Figure 19.</b> An undetermined product of lysated bacteria is able of increasing colonic afferent nerve discharge. ....	41
<b>Figure 20.</b> Chronic incubation with ultrapure LPS increases DRG neuronal excitability. ....	45
<b>Figure 21.</b> Standard-grade LPS applied acutely increases DRG neuronal excitability. ....	46
<b>Figure 22.</b> Effects of standard-grade LPS on excitability are not TLR4 mediated.	48
<b>Figure 23.</b> An undetermined product of lysated bacteria is capable of enhancing DRG excitability and colonic afferent nerve discharge.....	49
<b>Figura A1.</b> P2X5 en intestino de ratón.....	56
<b>Figura A2.</b> Exones de P2X5 de ratón. ....	57
<b>Figura A3.</b> P2X5 en intestino de cobayo. ....	58
<b>Figura A4.</b> Secuencia del cDNA del receptor P2X5.....	59
<b>Figura A5.</b> Exones del P2X5 de cobayo. ....	59
<b>Figura A6.</b> Alineamiento de la secuencia de amionoácidos (aa) del receptor P2X5 de ratón y cobayo. ....	60
<b>Figura A7.</b> Representación esquemática del gen <i>P2X5</i> de cobayo. ....	61
<b>Figura A8.</b> 5HT3A en intestino de cobayo. ....	62
<b>Figura A9.</b> Organización del gen que codifica para el 5HT3A de cobayo. ....	63

<b>Table 1.</b> Rome III Diagnostic Criteria: Functional constipation and Irritable Bowel Syndrome. ....	4
<b>Table 2.</b> Ligands for the Toll-Like Receptor-4 (TLR-4). ....	14
<b>Table 3.</b> Temperature and number of cycles used for PCR amplification of cDNA. ....	23
<b>Table 4.</b> Primers designed for amplification of each gene. ....	24

## ABBREVIATIONS

<b>5HT</b>	5 hydroxytryptamine
<b>ATP</b>	Adenosine Triphosphate
<b>BSA</b>	Bovine Serum Albumin
<b>cDNA</b>	Complementary DNA
<b>DMSO</b>	Dimethyl sulfoxide
<b>DRG</b>	Dorsal Root Ganglion
<b>dsRNA</b>	Double strand RNA
<b>DSS</b>	Dextran sulfate sodium salt
<b>FBS</b>	Fetal Bovine Serum
<b>GAPDH</b>	Glyceraldehyde 3-phosphate dehydrogenase
<b>GIPLS</b>	Glycolipids
<b>GRD</b>	Ganglio de la raíz dorsal
<b>HBSS</b>	Hank's Buffered Salt Solution
<b>IBD</b>	Inflammatory Bowel Disease
<b>IBS</b>	Irritable Bowel Syndrome
<b>I<math>\kappa</math>B</b>	$\kappa$ B Inhibitor
<b>IKK</b>	I $\kappa$ B Kinase Complex
<b>IL1-<math>\beta</math></b>	Interleukin 1 beta
<b>IL6</b>	Interleukine 6
<b>LBP</b>	LPS Binding Protein
<b>LCM</b>	Laser Capture Microdissection
<b>LPS</b>	Lipopolysaccharides
<b>LRR</b>	Leucine Rich Repeat
<b>MD-1</b>	Myeloid Differentiation 1
<b>MD-2</b>	Myeloid Differentiation 2
<b>mRNA</b>	Messenger RNA
<b>MyD88</b>	Myeloid differentiation primary response gene (88)
<b>NF-<math>\kappa</math>B</b>	Nuclear Factor $\kappa$ B
<b>NOD 1 and 2</b>	Nucleotide Binding Oligomerization Domain 1 and 2
<b>OCT</b>	Optimal Cutting Temperature
<b>ORF</b>	Open Reading Frame
<b>PAMPs</b>	Pathogen-Associated Molecular Patterns
<b>PBS</b>	Phosphate Buffered Saline
<b>PCR</b>	Polymerase Chain Reaction
<b>PRRs</b>	Pattern Recognition Receptors
<b>RHD</b>	Rel-Homology Domain
<b>RSVF</b>	Respiratory Syncytial Virus Fusion
<b>ssRNA</b>	Single strand RNA
<b>TBS</b>	Tris Buffered Saline
<b>TIR</b>	Toll IL-1 Receptor
<b>TLR</b>	Toll-like Receptor
<b>TNF-<math>\alpha</math></b>	Tumor necrosis Tumoral alpha
<b>UC</b>	Ulcerative Colitis
<b>UTR</b>	Untranslated Region
<b>B-ARAC</b>	$\beta$ - arabinofuranosylcytosine

## GLOSSARY

**Immunoreactivity.** Detection of an immune reaction between an antigen and an antibody.

**Inflammation.** Protective process in response to injury, infection or noxious stimulus, which will lead to repair and healing after of the destruction o removal of the injurious material.

**Lipopolysaccharides.** Also known as lipoglycans, are a large molecule consisting of a lipid and a polysaccharide joined by a covalent bond, they are found in the outer membrane of Gram-negative bacteria, act as endotoxins and elicit strong immune response in animals.

**Nociception.** Reception and transmission of pain signals in the nervous system.

**Ortholog gene.** Gene in different species that evolved from a common ancestral gene by speciation. Normally, orthologs retain the same function in the course of evolution.

**P2X Receptors.** Receptor membrane proteins activated by ATP, which include an ion channel.

**Toll-like Receptors.** They are a class of proteins that play a key role in the innate immune response, which recognize structurally conserved molecules derived from microbes.

## **ABSTRACT**

### **NEURONAL RECEPTORS INVOLVED IN THE INFLAMMATORY PROCESS**

This study examined whether bacterial cell products that might gain access to the intestinal interstitium could activate mouse colonic nociceptive dorsal root ganglion (DRG) neurons using molecular and electrophysiological recording techniques. Colonic projecting neurons were identified by using the retrograde tracer fast blue and Toll-like receptor (TLR) 1, 2, 3, 4, 5, 6, 9, adapter proteins Md-1 and Md-2, and MYD88 mRNA expression was observed in laser-captured fast blue-labeled neurons. Ultrapure LPS 1 g/ml phosphorylated p65 NF- $\kappa$ B subunits increased transcript for TNF- $\alpha$  and IL-1 and stimulated secretion of TNF- $\alpha$  from acutely dissociated DRG neurons. Moreover, lysate also activated afferent discharge from colonic mesenteric nerves, and this was significantly increased in chronic dextran sulfate sodium salt mice. These data demonstrate that bacterial cell products can directly activate colonic DRG neurons leading to production of inflammatory cytokines by neurons and increased excitability. Standard-grade LPS may also have actions independent of TLR signaling.

#### **KEY WORDS:**

Lipopolysaccharide; NF- $\kappa$ B; Sensory neuronal excitability, Multiunit activity, Dorsal root ganglia

## RESUMEN

### ESTUDIO DE RECEPTORES NEURONALES INVOLUCRADOS EN EL PROCESO INFLAMATORIO

Este estudio examinó si los productos celulares bacterianos que podrían tener acceso al intersticio intestinal podrían activar las neuronas nociceptivas colonicas de ganglios de la raíz dorsal (GRD) de ratón utilizando técnicas moleculares y de registro electrofisiológico. Las neuronas con proyecciones colonicas fueron identificadas usando el marcador retrogrado azul rápido; y la expresión de RNAm del receptor tipo Toll (TLR) 1, 2, 3, 4, 5, 6 y 9, las proteínas adaptadoras MD1 y MD2 y MYD88 fueron observados en neuronas marcadas con azul rápido capturadas por láser. 1 µg/ml de LPS grado ultrapuro incrementó el transcrito de TNF- $\alpha$  y IL-1 $\beta$  y estimuló la secreción de TNF- $\alpha$  de neuronas disociadas de GRD. Por otra parte, el lisado de *E. coli* incrementó significativamente la actividad basal de los nervios aferentes mesentéricos y en ratones con un tratamiento crónico DSS. Estos datos demuestran que los productos celulares bacterianos pueden activar directamente las neuronas de GRD colónicas llevando a la producción de citocinas inflamatorias e incrementando su excitabilidad. El LPS grado estándar pudiera también tener acciones independientes de la señalización de TLR.

#### **PALABRAS CLAVE:**

Lipopolisacáridos; NF- $\kappa$ B; Excitabilidad neuronal sensorial, Actividad Multiunitaria, Ganglio de la raíz dorsal.

## **I. GENERAL BACKGROUND**

The Inflammatory Bowel Disease (IBD) and the Irritable Bowel Syndrome (IBS) are among the most common intestinal disorders in northern countries. Although, its incidence and prevalence in southern countries is much lower (68). IBD (includes Crohn's disease and ulcerative colitis [UC]) is associated with a measurable inflammatory response leading to gut tissue damage (75). IBS patients, on the other hand, display in some cases only low-grade colonic mucosal inflammation (12). However, IBD and IBS have a common symptom, the pain, which will be the focus of this thesis.

### *Inflammatory Bowel Disease*

The etiology of IBD is unknown but most researchers accept that it is the result of a chronic and excessive mucosal immune response (21). Thus, a chronic inflammation of the gastrointestinal tract is a characteristic in IBD (49). However, patients with IBD may eventually present all or some of the following symptoms: diarrhea, weight loss, cachexia, rectal bleeding, fever, fatigue, disrupted digestion, and abdominal pain. Some patients may have remission periods when the inflammation tends to be minimal. The principal difference between the Crohn's disease and the ulcerative colitis is the extension and location of the inflammation. Thus, while in the ulcerative colitis is restricted to the colon, in the Crohn's disease the inflammation can be found throughout the whole gastro-intestinal tract but most commonly in the distal ileum and colon (49, 75).



The excessive mucosal immune response seen in IBD is likely the result of an interaction between immunological, environmental and genetic factors (70). Some studies suggest that the first event in the disease is the result of a dysregulated inflammatory response rather than an aggressive inflammatory response by a defective intestinal immune system (6). Thus, it is possible that the immune response is exacerbated by the presence of potential enteric antigens from luminal bacteria, viruses, or food allergens (51).

The treatment of IBD could be integrated by the administration of one or more of the next therapeutic options: antibiotics, systemic or local steroids, immunomodulators, biologic agents, selective adhesion molecule inhibitors, stimulation immune, and probiotics. In the case of the administration of a specific medication type, this could vary if the treatment is for Chron's disease or ulcerative colitis. It is important to point that so far the cure for IBD is unknown but, when properly treated, it can be maintained in remission for long periods (48).

### *Irritable Bowel Syndrome*

Another disease associated with the inflammatory bowel disease is the irritable bowel syndrome (IBS), a disease very common among the diagnostics of intestinal diseases. IBS is a moderated intestinal chronic disease that is frequently accompanied by abdominal pain and altered intestinal motility, resulting in either diarrhea or constipation, as well as an elevation of visceral pain and hypersensitivity (69). Some researches suggest that gut motility is involved and this might result from a different intestinal microflora in IBS patients, the facultative microorganisms tend to increase whereas the lactobacilli to decrease (56).

The symptoms cannot be explained, in most cases, by structural or biochemical abnormalities, however, sometimes a low grade mucosal inflammation especially in post-infectious IBS is observed (38). Because disease-specific biomarkers are absent, the diagnosis of IBS is based on the Rome III diagnostic criteria (20), which is listed on Table 1. Thus, IBS diagnosis is established in terms of multiple physiological determinants contributing to a common set of symptoms rather than a single disease entity (24).

The IBS have a prevalence of 10 to 15% in the general population being one of the most common functional gastrointestinal disorders worldwide (12). The incidence and prevalence of the disease in Mexico, as a country, is unknown but in 3 medical centers of Mexico city, 21% of patients who requested consultation for any gastrointestinal discomfort, were found to be suffering IBS (17).

Currently, therapy for IBS includes a wide variety of pharmacologic agents and nonpharmacologic methods. Among the first group are included opioid derivatives, laxatives, antidepressants, anticholinergic or antispasmodic drugs and serotonin receptor modulating agents. Other therapeutic measurements include an increased fiber intake during constipation, obviate fermenting foods, reduced fat intake and psychological treatment; all of the above have resulted useful for patients with IBS (49).

**Table 1.** Rome III Diagnostic Criteria: Functional constipation and Irritable Bowel Syndrome.

Symptoms  $\geq 3$  months; onset  $\geq 6$  months prior to diagnosis

Functional Constipation	IBS
<ul style="list-style-type: none"> <li>• Must include <math>\geq 2</math> of the following:               <ul style="list-style-type: none"> <li>– Straining*</li> <li>– Lumpy or hard stools*</li> <li>– Sensation of incomplete evacuation*</li> <li>– Sensation of anorectal obstruction/blockage*</li> <li>– Manual maneuvers to facilitate defecation (eg, digital evacuation, support of the pelvic floor)*</li> <li>– <math>&lt; 3</math> defecations/wk</li> </ul> </li> <li>• Loose stool rarely present w/o use of laxatives</li> <li>• Insufficient criteria for IBS</li> </ul>	<ul style="list-style-type: none"> <li>• IBS: Recurrent abdominal pain/discomfort <math>\geq 3</math> d/month for the past 3 months, associated with <math>\geq 2</math> of the following:               <ul style="list-style-type: none"> <li>– Improvement with defecation</li> <li>– Onset associated with change in stool frequency</li> <li>– Onset associated with change in stool form</li> </ul> </li> <li>• IBS is subtyped by predominant stool pattern               <ul style="list-style-type: none"> <li>– IBS-C: hard or lumpy stools<math>\dagger</math> <math>\geq 25\%</math> of defecations; loose or watery stools<math>\ddagger</math> <math>&lt; 25\%</math> of defecations<math>\S</math></li> </ul> </li> </ul>

\* $\geq 25\%$  of defecations.  $\dagger$ Bristol Stool Form Scale 1–2: separate, hard lumps like nuts (difficult to pass); or lumpy, sausage-shaped stool.  $\ddagger$ Bristol Stool Form Scale 6–7: fluffy pieces of stool with ragged edges; mushy stool; or watery w/out solid pieces (entirely liquid).  $\S$ In the absence of use of antidiarrhoeal or laxatives. Based on: Longstreth GF et al. *Gastroenterology*. 130:1480-1491, 2006.

### *Intestinal diseases and pain*

Abdominal pain is reported is likely the most debilitating and complex symptom present in both, IBD and IBS (21) and therefore, this will be the focus of the present thesis.

### *Pain*

The sensation of pain is the most distinguished of all the sensory modalities. Inside the pain sensations, we found pricking, soreness, aching, burning and stinging.

The pain is considered a submodality of somatic sensation as pressure, touch and position sense and have a primordial protective function: pain is a common symptom of injuries and illness so that it is considered a warning of something that should be avoided or treated (45). The intensity of pain is affected by internal and external factors, thus, the same stimulus can produce different responses in different individuals under the same conditions (45).

The mechanism through which the pain signal is sent to the central nervous system is known as nociception. The nociceptors have the ability to relay this information indicating its location, nature and intensity of the pain. The cell bodies of those nerve terminals that innervate the intestine or colon are contained within the dorsal root ganglia (DRG) and they are known as primary sensory neurons (44).

Nociceptive neurons can be classified into three groups based on functional and anatomical criteria. A $\beta$  primary sensory fibers have big bodies and their axons are myelinated and rapidly conducting, however most of these fibers detect innocuous stimuli, so they do not contribute to pain (23). Furthermore, C fibers (small cell body) unmyelinated slowly conducting and the A $\delta$  fibers (medium cell body) slightly myelinated conducting faster, giving rise to most of nociceptors (67). It has long been assumed that the 'first' and 'second' pain are mediated by A $\delta$  and C nociceptors, respectively, namely the rapid, acute, sharp pain and the delayed, more diffuse, dull pain evoked by noxious stimuli (Figure 1) (45).

### *Nociceptive pathway*

Nociception is the process by which the pain signal is sent to the central nervous system. There are three neurons involved in the nociceptive pathway: i) the primary sensory neuron (first order), the secondary neuron (second order or spinothalamic), and the tertiary neuron (third order) (2). This last neuron projects to the primary sensory cortex. The body of the primary sensory neurons is located in the dorsal root ganglia or in the trigeminal ganglia. These neurons are called "T" cells because a single cell process arises from their soma, which splits to form two branches: a central (that enters into the central nervous system) and a peripheral one (that innervates the tissues). The intestine is innervated for the thoracic dorsal root ganglia T10, T11, and T12. When a noxious stimulus activates the nociceptor terminals, the signal is transmitted through the branches of the first neuron to the second order neuron, which soma is located in the posterior horn of the spinal cord. The somas of these neurons generate an axon that crosses the spinal cord and forms the spinothalamic tract. These axons make synapses with third order neurons located in the thalamus. The third-order neuron sends the signal to cortical neurons, where conscious perception of pain occurs (Figure 2) (14).

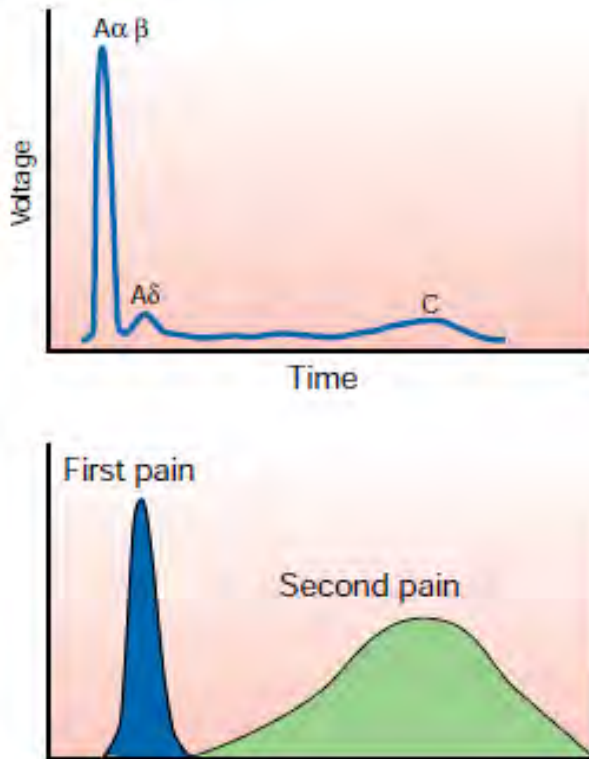


**Figure 1. Different nociceptive neurons detect different modalities of pain.** It is well known that conduction velocity is directly related to fiber diameter and this is highlighted in the compound action potential recording from a peripheral nerve. Most nociceptors are either A $\delta$  or C fibres, and their different conduction velocities (6-25 and 1.0 m/s, respectively) account for the first (fast) and second (slow) pain responses to injury, see lower graph (44).

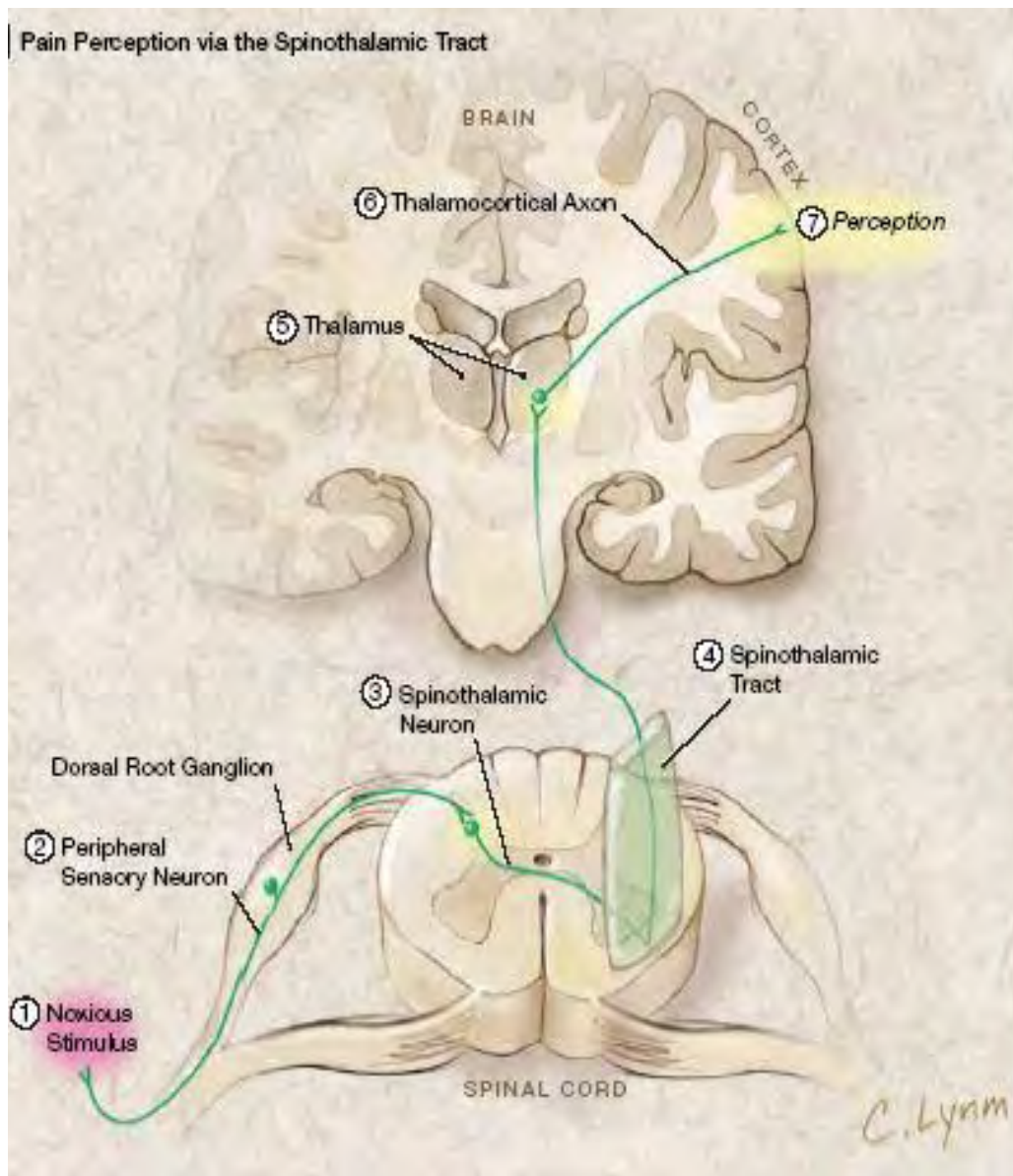


**Figure 2. Scheme of the nociception pathway.** A noxious stimulus (1) active peripheral sensory neurons, "T" neurons (2), that synapse on spinothalamic tract neurons (3), which axons travel on the contralateral spinal cord as the spinothalamic tract (4) to synapse with neurons in the thalamus (5). From here, thalamocortical axons synapse on cortical neurons, in the primary sensory cortex, resulting in conscious perception of pain (42).

## *Pain and Inflammation*

Noxious stimuli required a minimal intensity to lead nociception, which is known as pain threshold. Above this, nociceptive nerve endings will signal pain to the brain cortex. This threshold is influenced by a variety of conditions, including injury and a variety of inflammatory mediators. Figure 3 shows pain intensity as a function of the stimulus intensity in normal condition and after damaging the same tissue. Notice that the injury lowers the threshold and therefore, an innocuous stimulus can now excite nociceptors and cause a painful sensation (allodynia). In addition, a stimulus that was previously painful now evokes a greater degree of pain, which is known as hyperalgesia (8, 54).

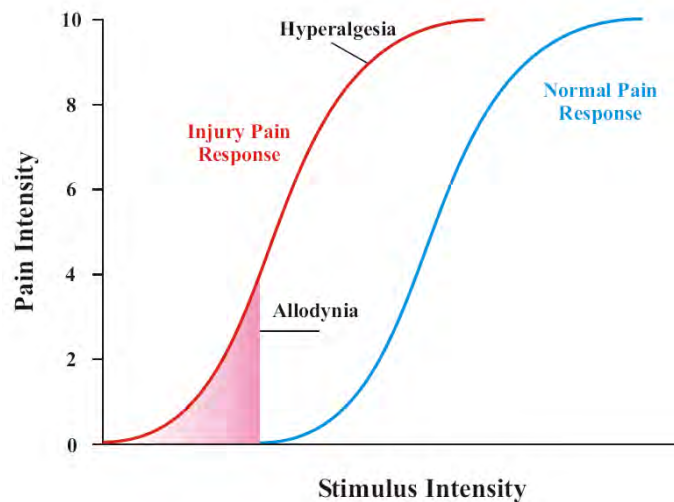


**Figure 3. Graphical representation of the hyperalgesia and allodynia concepts.** In hyperalgesia, more pain is reported in response to a given noxious stimulus. Allodynia is noticed when an innocuous stimulus (e.g. touching) is able to induce pain (8).

Hyperalgesia and allodynia are determined by changes in the properties of nociceptive neurons (e.g. their ion channels, membrane receptors, gene



expression) responsible for generating and relaying nociceptive information to the central nervous system (54). These neuronal changes are mediated by inflammatory cells and inflammatory mediators (32).

The inflammation is a protective pathologic process consisting of a dynamic complex characterized of histologically and cytologic changes, cellular infiltration, and mediator release. It occurs in the affected blood vessels and adjacent tissues in response to injury, irritation, infection or abnormal stimulation caused by a physical, chemical, or biologic agent, resulting in morphologic and functional characteristic changes. These so-called cardinal signs of inflammation are: redness, heat (or warmth), swelling, pain, and sometimes a fifth sign, lost of function (21). The destruction or removal of the injurious material will lead to repair and healing (59).

In the gut there are many particles that promote inflammation; some of these are known like pathogen-associated molecular patterns (PAMPs). Many of these come from bacteria or viruses present in the intestine. Receptors that recognize PAMPs are part of the host innate immunity and were selected by evolution to recognize pathogen-derived components that are critical for the survival of the pathogen (13) and (27). These receptors are known as pattern recognition receptors (PRRs). Toll-like receptors (TLRs) are one of the receptors families that identify PAMPs. Activation of metabolic pathways by PAMPs leads to the release of cytokines that can promote or decrease inflammation (15). The intestine has the largest variety of these receptors that modulate the production of pro- and antiinflammatory cytokines and would permit a fine balance between both types of cytokines.

### *Toll Like Receptor (TLR)*

The immune system is alerted to the presence of invading pathogens by signaling through of PRRs as TLRs (28). These receptors (Figure 4) are a family of type I transmembrane proteins that possess a N-terminal leucine-rich-repeat (LRR) domain on tandem, which is typically 24-29 residues in length, a sequence likely to form a single transmembrane helix and a C-terminal cytoplasmatic signaling domain known as Toll IL-1 receptor (TIR) domain (77).

Thirteen mammalian TLRs, 10 in humans and 12 in mice have been identified (9). The first nine TLRs are found in humans and mice whereas TLR10 is present only in humans and TLR11 only in mice. The ligands and signaling pathways of the TLRs 1-9 and 11 (Figure 5) are well known whereas the biological role(s) of TLRs 10, 12, and 13 remain unclear, as their expression patterns, ligands, and modes of signaling have yet to be identify (77).

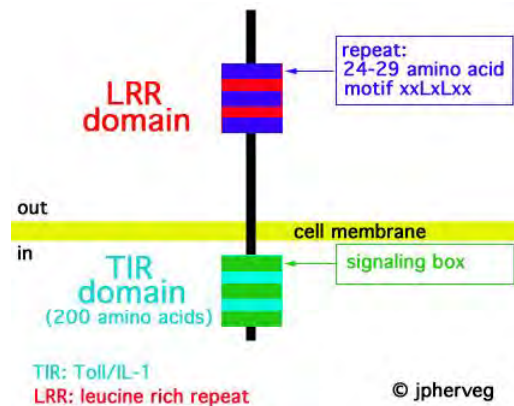


**Figure 4. Structure of the Toll Like Receptors (TLRs) includes a leucine-rich repeat (LRR) and a Toll/IL-1R (TIR) domain.** The members of the TLRs family share a significant homology in the cytoplasmic region, the TIR domain of ~200 amino acids. In the extracellular portion contain a LRR motif that consists of varying numbers of repeats. Each repeat is 24-29 amino acids in length, containing the motif xxLxLxx. LRR domains are involved in pathogens recognition (41).

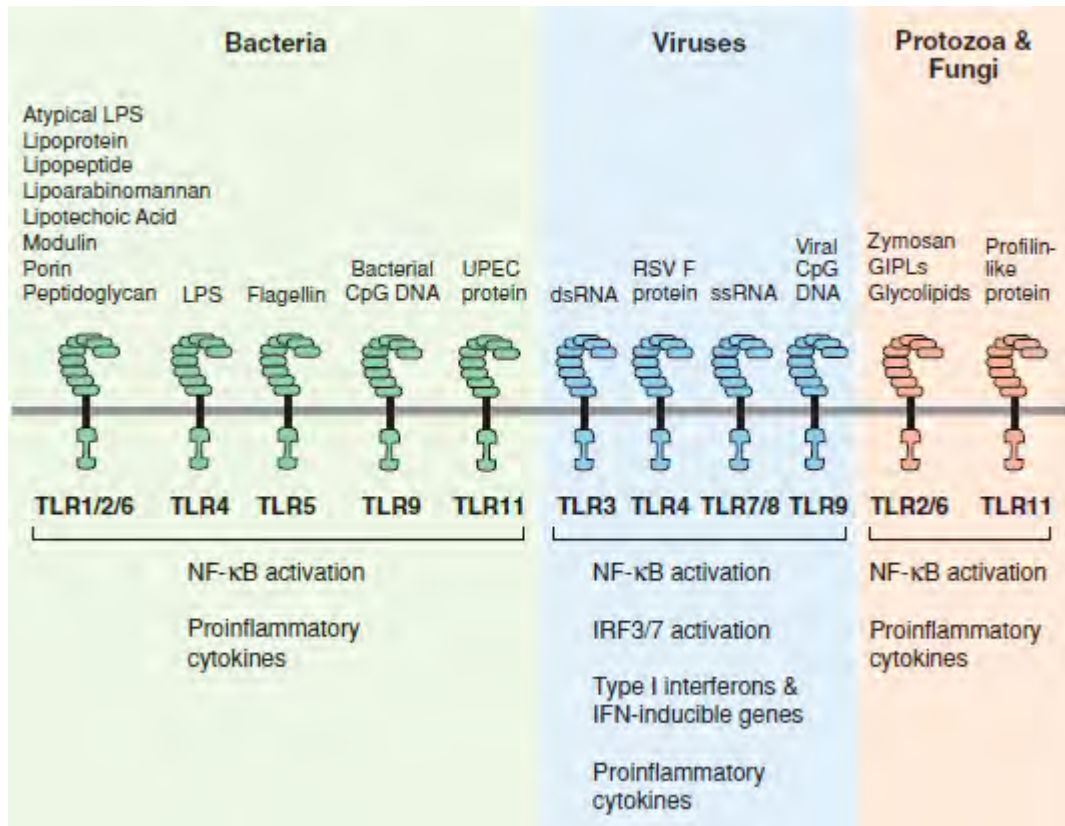


**Figure 5. Toll-like Receptors (TLRs) ligand specificities.** TLRs recognize a diverse array of pathogen-associated molecular patterns (PAMPs) from bacteria, viruses, protozoa, and fungi. For detection of bacteria, heterodimeric TLR2/1 binds triacyl lipopeptides, whereas TLR2/6 dimers bind diacyl lipopeptides and lipoteichoic acid. Homodimeric TLR2 binds peptidoglycan, atypical LPS, phenol-soluble modulin from *Staphylococcus epidermidis*, and porin proteins from *Neisseria*. In addition, TLR4 binds LPS, TLR5 binds flagellin, and TLR9 binds bacterial CpG DNA. TLR11 detects an unidentified protein(s) from uropathogenic *Escherichia coli*. Viral dsRNA, RSV F protein, ssRNA and unmethylated CpG DNA are sensed by TLRs 3, 4, 7/8, and 9, respectively. Finally, heterodimeric TLR2/6 binds fungally derived zymosan and *Trypanosoma cruzi* GIPLs, whereas TLR11 also senses a profilin-like protein from *Toxoplasma gondii*. Abbreviations: dsRNA, double-stranded RNA; LPS, lipopolysaccharide; GIPLs, glycolipids; PAMP, pathogen-associated molecular pattern; RSVF, respiratory syncytial virus fusion; ssRNA, single-stranded RNA; TLR, Toll-like receptor” (77).

### *Toll-like receptor 4 (TLR4)*

The lipopolysaccharides (LPS) are the most abundant compound in the cell wall of Gram-negative bacteria and are the most studied *TLR*-ligand (58). Trace concentrations of LPS can activate the innate immune system via *TLR4*, which induces the production of proinflammatory mediators, including cytokines like Tumoral Necrosis Factor- $\alpha$  (TNF- $\alpha$ ), Interleukine-1 (IL-1), and Interleukine-6 (IL-6) (77). Unlike the others receptors of the *TLR* family, *TLR4* need additional components of the LPS recognition complex to obtain a robust response, among these are LPS-binding protein (LBP), MD-2 (Myeloid Differentiation protein - 2), and CD14 (Figure 6) (53).

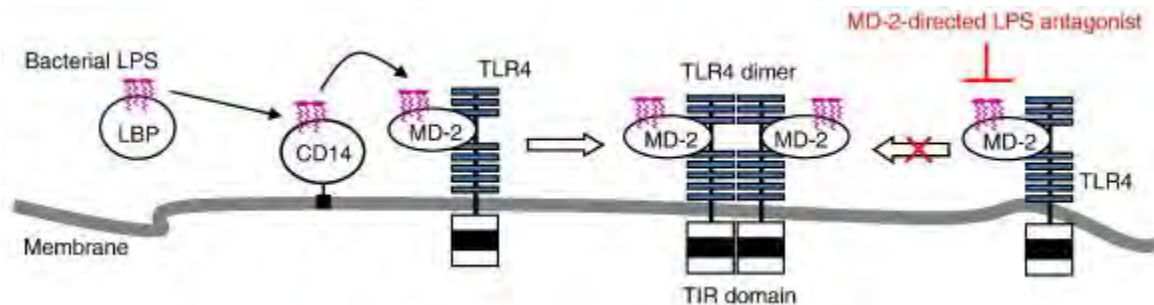


**Figure 6. Schematic representation of lipopolysaccharides (LPS) trafficking.** A serum protein LPS-binding protein (LBP) transfers bacterial LPS to CD14. CD14 concentrates LPS molecules and presents LPS monomers to a receptor complex of MD-2 and TLR4. The MD-2/TLR4 complex bound with LPS is converted to a receptor multimer of (LPS-MD-2-TLR4), an activation index TLR4 mediated inflammatory cascade. Modified of (65)

LPS first bind to LBP protein, which is free in serum, subsequently transferred to the CD14 protein that is anchored to the membrane. CD14 is responsible for concentrating the LPS molecules and transferred to MD-2 protein,

which is complexed to the TLR-4 receptor. It is necessary to carry out these transfer steps of LPS to obtain a complex functional MD-2/TLR-4 otherwise, if the LPS binds directly to MD-2, is a repressor or antagonizing effect. LPS is not only ligand that activates the receptor TLR4, others such as lipid A analogs, taxol, mycobacterial components, etc, also activate the receptor (Table 2) (77).

**Table 2.** Ligands for the Toll-Like Receptor-4 (TLR-4).

Ligands	Origin of ligands
LPS	Gram-negative bacteria
Flavolipin	<i>Flavobacterium meningosepticum</i>
ER-112022, E5564, E5531	Synthetic compounds
Taxol	Plant
Fusion protein	Respiratory syncytial virus
Envelope proteins	Mouse mammary tumor virus
Hsp60	<i>Chlamydia pneumoniae</i>
Hsp60	Host
Hsp70	Host
Type III repeat extra domain A of fibronectin	Host
Oligosaccharides of hyaluronic acid	Host
Polysaccharide fragments of heparan sulfate	Host
Fibrinogen	Host
$\alpha$ A crystallin and HSPB8	Host (recombinant <i>E. coli</i> -produced proteins)

Table modified (27).

### *Pathway of signaling*

NF- $\kappa$ B is an important transcription factor that replies to diverse cell stimuli by activating the expression of stress response genes. Multiple signals, including cytokines, engagement of the T-cell receptor, bacterial and viral products induce NF- $\kappa$ B transcriptional activity (35). In mammalian cells, there are five NF- $\kappa$ B family members, RelA (p65), RelB, c-Rel, p50/p105 (NF- $\kappa$ B1) and p52/p100 (NF- $\kappa$ B2),

and different NF- $\kappa$ B complexes are formed from their homo and heterodimers bound to I $\kappa$ B family members (66). The NF $\kappa$ B family members have an N-terminal domain of approximately 300 amino acids called the Rel-homology domain (RHD), which mediates DNA binding and dimerization. Also, Rel family members, contain C-terminal transcriptional activation domain (Figure 7) (36).

In cells without stimulation, the transcription factor NF- $\kappa$ B is found in the cytosol in an inactive form bound to  $\kappa$ B inhibitor (I $\kappa$ B). Activation of the I $\kappa$ B kinase complex (IKK) carries out degradation of I $\kappa$ B, releasing NF $\kappa$ B, which is translocated to the nucleus and induces transcription of pro-inflammatory genes (29), pathway include the participation of others proteins show in Figure 8.

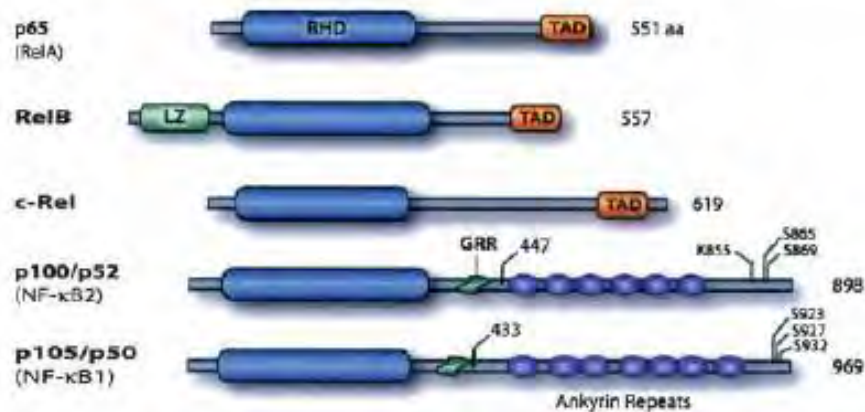


**Figure 7. Schematic representation of NF- $\kappa$ B family proteins.** Members of the family of NF- $\kappa$ B family proteins are shown. The number of amino acids in each protein is indicated on the right. Presumed sites of cleavage for p100 (amino acid 447) and p105 (amino acid 433) are shown. Phosphorylation and ubiquitination sites on p100 and p105 are indicated. (*RHD*) *Rel* *homology domain*; (*TAD*) *transactivation domain*; (*LZ*) *leucine zipper domain*; (*GRR*) *glycine-rich region* (36).

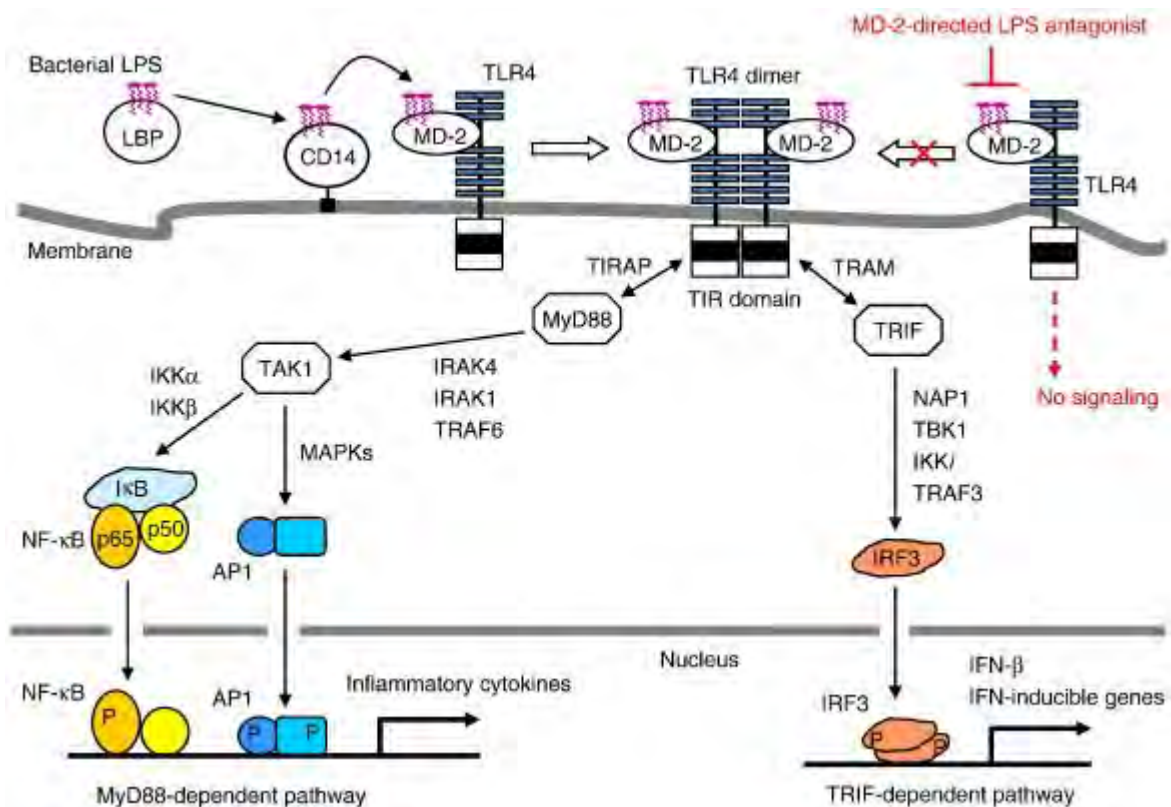


**Figure 8. Schematic diagram of LPS trafficking and TLR4-mediated inflammatory signaling in the mammalian host.** TLR4 signaling is diverged into MyD88-dependent and TRIF-dependent pathways. Intracellular adaptor molecules are TIRAP (TIR domain-containing adaptor protein), MyD88, TRAM (TRIF-related adaptor molecule), and TRIF. MyD88-dependent pathway activates the transcription factors of NF- $\kappa$ B and AP1 for the induction of inflammatory cytokines through multiple signaling molecules such as IRAK4 (IL-1 receptor-associated kinase 4), IRAK1, TRAF6 (TNF receptor-activated factor 6), TAK1 (transforming growth factor- $\beta$ -activated kinase 1), IKK $\alpha$  (inhibitory  $\kappa$ B kinase  $\alpha$ ), IKK $\beta$ , and MAPKs (mitogen-activated protein kinases). TRIF-dependent pathway activates the transcription factor of IRF3 for the up-regulation of IFN- $\beta$  and IFN-inducible genes through NAP1 (NF- $\kappa$ B-activating kinase-associated protein 1), TBK1 (TRAF family member-associated NF- $\kappa$ B activator-binding kinase 1), IKK $i$ , and TRAF3. Image obtained of (65).

### *Direct Background*

Maintaining homeostasis in the gastrointestinal tract is more complicated than in any other part of the body because only a barrier of epithelial cells separates the *internal medium* from the lumen, which might contain a microbial flora. The permeability of the mucosa and the response to the bacterial flora is determined by regulatory systems of the mucosal immune system and abnormalities in this results in acute or chronic inflammatory processes (4, 21, 63). Studies confirm that microbiota in patients with IBD and IBS seem to be characterized by: i) high concentrations of bacteria in contact with the mucosa, ii) the presence of high numbers of unusual bacteria, iii) instability and a reduction in the biodiversity of 30 to 50%, and iv) a high concentration of pathogens. Biodiversity in microbiota is believed to be desirable because it generates higher resistance to pathogens (56, 71, 72, 75).

In basal conditions, the enterocyte TLR signaling may contribute to intestinal homeostasis. However, when there is exposure to physiological stressors, like infection, hypoxia, or exposure to high concentrations of LPS, TLR signaling can lead to deep and harmful effects on the epithelial monolayer, including the release of proinflammatory cytokines, the generation of epithelial damage by apoptosis, and stop intestinal repair. As a result, barrier failure occurs, leading to the development of bacterial translocation and intestinal inflammation (31).

Effect of LPS and the activation of TLR4 have been studied in many different cell types (40, 55), including rat and human myenteric neurons, and rat trigeminal sensory neurons (5, 7, 22). TLR4 immunoreactivity is present in mouse myenteric (more of 90%) and DRG (40%) neurons (1, 7).



*The rationale behind this study*

It has been demonstrated the presence and activation TLR4 receptor in several types of neurons, including DRG sensory neurons. DRG nociceptive neurons that innervate the colon express the proteins necessary to form a functional TLR4 receptor, so it is possible that these neurons are capable of detecting pathogens particules when the integrity of the epithelial barrier is altered. Which might contribute to nociception and hyperalgesia.

## **II. HYPOTHESIS**

If the epithelial barrier permeability increases, the passage of bacterial products or bacteria may directly signal to nociceptive neurons that innervate the mouse colon.

## **III. GENERAL AIM**

To investigate if LPS induces activation of NF- $\kappa$ B pathway in mouse primary nociceptive neurons.

### *Specific objectives*

- Verify the expression of TLR family receptors in mouse primary nociceptive neurons by RT-PCR.
- Determine whether LPS activates NF- $\kappa$ B pathway in neurons in culture through western blot technique, and whether this activation depends on time and concentration of LPS.
- Verify the transcription of some target genes of the pathway as TNF- $\alpha$ , IL-1 $\beta$  and IL-6 using RT-PCR and quantify the production of cytokine TNF- $\alpha$  by ELISA.
- Quantify the effect of the LPS application on the mesenteric nociceptors of the colon.
- Compare the results using standard grade LPS and ultrapure LPS.

#### IV. MATERIAL AND METHODS

##### *Animals and Cell Cultures*

Male CD-1 mice between 25-30 g were used (from Charles Rivers Laboratories) to obtain sensory neurons from DRG (T9-T13) (Figure 9). Neurons were enzymatically dissociated by incubation for 25 min with two treatments, first with 60 U of papain plus 12  $\mu$ g L-cysteine and 3  $\mu$ l saturated  $\text{NaHCO}_3$  in 1.5 ml of HBSS. The enzyme was removed and a second treatment was used with 12  $\mu$ g of collagenase and 14  $\mu$ g of dispase in 3 ml of HBSS, both incubated at 37 degrees. After washing with F-12 medium containing 10% fetal bovine serum (FBS), the DRGs were triturated and the cell suspension was pelleted by centrifugation at 2,000 rpm for 5 min. To remove most of the nonneuronal cells (1), the pellet was resuspended in HBSS with 20% Percoll gradient, and centrifugated at 2,500 rpm for 7 min. The supernatant containing nonneuronal cells was discarded and the neurons were washed with HBSS and pelleted by centrifugation at 2000 rpm for 5 min. The final pellet enriched with neurons was suspended in F-12 medium plus FBS, penicillin/streptomycin and 10  $\mu$ M  $\beta$ -arabinofuranosylcytosine ( $\beta$ -ARAC) and plated in poly-D-lysine/laminin-coated 17-mm tissue culture dishes. Dissociation and culturing procedures have previously been described (57). LPS was added to the cell culture for the time previous required to fulfill 21 hr of total culture time. Figure 10 shows a flow chart describing the general experimental protocols used.

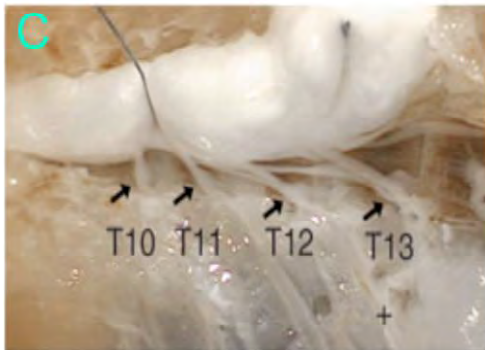
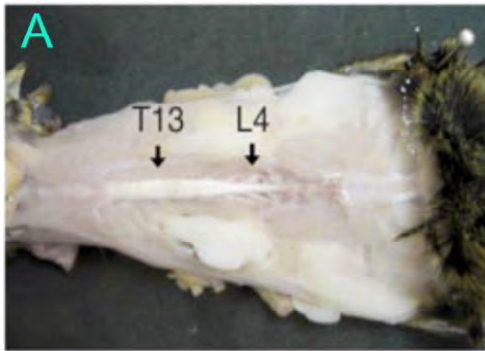


**Figure 9. Photographs of the dorsal root ganglia (DRGs) corresponding to the T9-T13 spinal segments.** Panel (a) shows the segmental distribution of the ganglia within the mouse; panels (b–c) are magnified views revealing the location of the ganglia at different segmental levels. Arrows point to ganglia. The last thoracic ganglion (T13) and the ganglion with the greatest contribution to the sciatic nerve (L4) are identified for orientation with respect to the whole mouse (a). Thoracic ganglia are revealed here using pins to pull back the spinal cord (b). The thoracolumbar transition is easily identified because T13 is just caudal to the last rib (+ sign) (c). Image taken y modified of Malin et al., 2007.

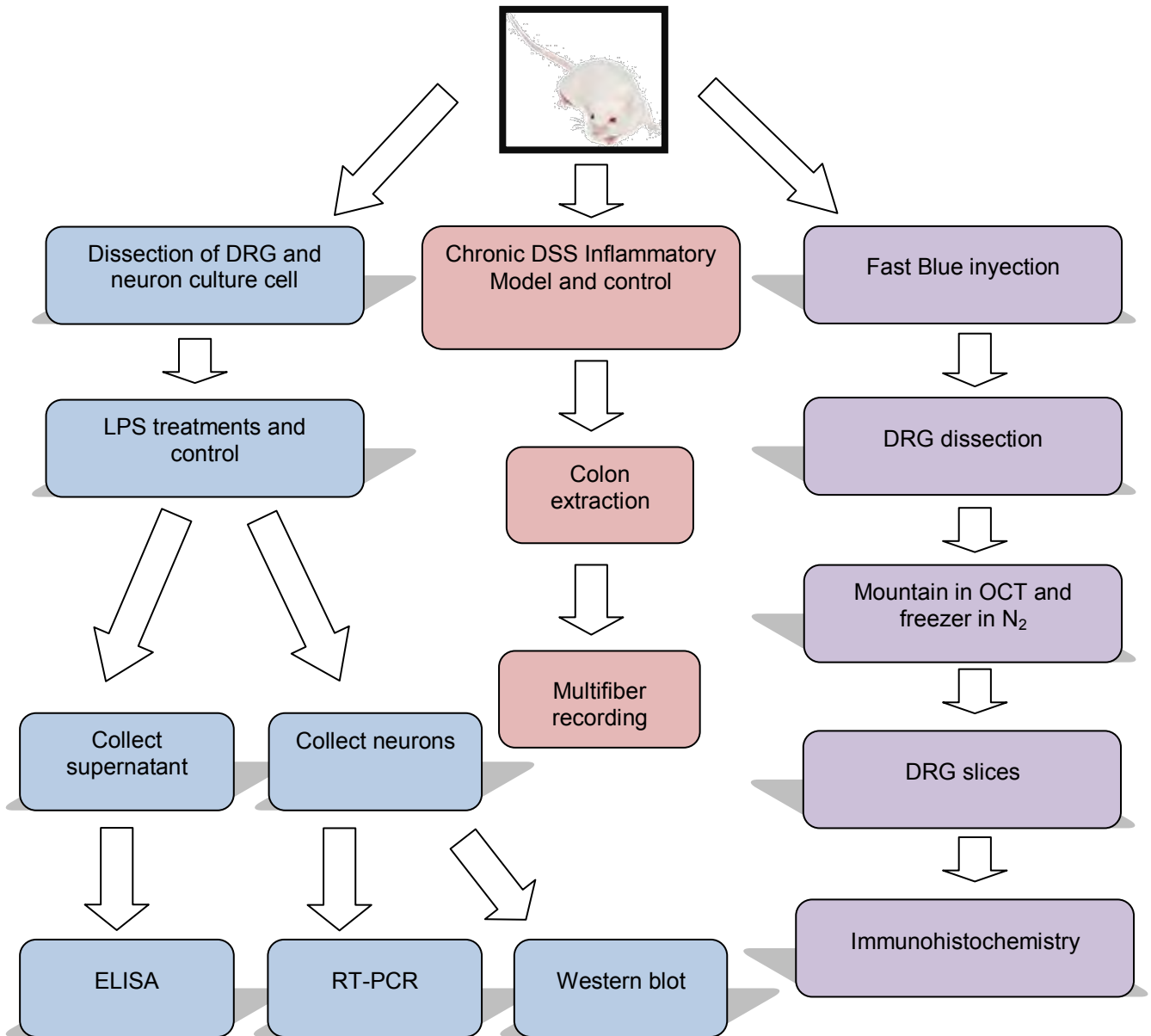


**Figure 10. Chart Flow of Experimental Protocols.**

### *Semiquantitative RT-PCR*

RT-PCR semiquantitative technique was used to determine the relative neuronal mRNAs levels for TNF- $\alpha$ , IL-6, IL-1 $\beta$ , NF $\kappa$ B and GAPDH. Total mRNA was obtained using Trizol Reagent (Invitrogen, Carlsbad, USA). cDNA was synthesized from 0.5  $\mu$ g total RNA with Oligo dT and SuperScript III (Invitrogen, Carlsbad, USA) for 50 min at 50°C. cDNA (0.5  $\mu$ l) was used as a template for PCR amplification in

a 25  $\mu$ l reaction volume containing 2.5  $\mu$ l buffer 10x, 200 nM dNTP's, 1.5 mM MgCl, 0.2  $\mu$ M of each primer and 0.1  $\mu$ l taq DNA polymerase (Invitrogen, Carlsbad, USA). The reaction conditions for each pair of primers are indicated in Table 3.

**Table 3.** Temperature and number of cycles used for PCR amplification of cDNA.

Gene	Cycles	Annealing °T	Extension time to 72°C
TNF- $\alpha$	38	62	30 s
GAPDH	35	61.5	30 s
NFkB	38	61.5	40 s
IL-1 $\beta$	38	61.5	30 s
IL6	38	61.5	60 s
TLR1	35	60	20 s
TLR2	35	58	20 s
TLR3	35	56	20 s
TLR4	38	63	50 s
TLR5	35	60	20 s
TLR6	35	58	20 s
TLR9	35	58	20 s
MyD88	35	62	20 s
Md1	35	60	20 s
Md2	35	60	20 s
Nod1	35	58	20 s
Nod2	35	60	20 s

All primers used to obtain the PCR products were obtained from Sigma and are listed in Table 4. Ethidium bromide was used for staining the gels.

**Table 4.** Primers designed for amplification of each gene.

Gene	Size, pb	Sense	Antisense
TNF- $\alpha$	435	CTTGTCTACTCCCAGGTTCTCTTCA	ACTCTGAGCCATAATCCCCTTTCT
GAPDH	489	GTCGTGGAGTCTACTGGTGTCTTC	GTCATCATACTTGGCAGGTTTCTC
NF $\kappa$ B	620	GATTCGATTCCGCTATGTGTG	TCCTGCTGTTCTGTCCATTCTC
IL-1 $\beta$	505	AGGAGAACCAAGCAACGACA	ATCAGAGGCAAGGAGGAAA
IL6	538	CTTCCATCCAGTTGCCTTCTT	GGTCCTTAGCCACTCCTTCTGT
TLR1	185	GTGTGCAGCTGATTGCTCAT	CAAACCGATCGTAGTGCTGA
TLR2	199	AAGAGGAAGCCCAAGAAAGC	CGATGGAATCGATGATGTTG
TLR3	219	TCGGATTCTTGTTTTCAAGG	TTTCGGCTTCTTTTGATGCT
TLR4	201	ACCTGGCTGGTTTACACGTC	CTGCCAGAGACATTGCAGAA
TLR5	193	GCCACATCATTTCCTCCT	ACAGCCGAAGTTCCAAGAGA
TLR6	189	CCAAGAACAAAAGCCCTGA	GTTTTGCAACCGATTGTGTG
TLR9	195	TGCTTTGGCCTTTCCTCTT	AACTGCGCTCTGTGCCTTAT
MyD88	217	TGGCCTGAGCAACTAGGACT	CGTGCCACTACCTGTAGCAA
Md1	282	CCTATCCCCTTTGTGAGGAG	CTTGGTTATCAGTGGTTCTTGC
Md2	250	GACGCTGCTTCTCCATA	CTTACGCTTCGGCAACTCTA
Nod1	212	GAAATTGGCTTCTCCCCTTC	CTGCCAGGTTTTTCATTGTT
Nod2	193	AGGGCATCCAAGTGTACCTG	TACATGTCCGTGCTGGTTGT

### *Western Blotting*

A standard protocol of Western blot was used to examine the expression of NF $\kappa$ B, pNF $\kappa$ B, SNAP25, P38 and pP38 in cultured DRG neurons from CD-1 mice. The harvested neurons (from 3 mice) were lysed in Trizol Reagent (Invitrogen,

Carlsbad, USA) and the final pellet was diluted in Lysis Samples Roger's Buffer, supplemented with Complete Protease-Inhibitor Cocktail (Roche Molecular Biochemicals, South Essex, United Kingdom), heated at 95 degrees for 5 minutes, and stored at -20 degrees. The protein amount was quantified using the Micro BCA (Bicinchoninic Acid) Protein Assays Kit (The Thermo Scientific, Rockford, USA) and 40 µg of total protein samples were run in each lane of SDS-PAGE gels (10% gels). Protein were blotted onto PVDF (Polyvinylidene fluoride) membranes (Immobilon-P), and later were incubated for 2 hrs at environmental temperature in a dilution 1:1000 of primary antibody, the membrane was washed and later incubated for 1 hr in the secondary antibody. The proteins were detected using the SuperSignal West Pico Chemiluminescent Substrate (The Thermo Scientific, Rockford, USA)

#### *Fast Blue Injection*

Mice were anesthetized with ketamine-xylazine (0.15/0.01 mg/g wt ip) and subjected to midline laparotomy (10), the colon was exposed, and the retrograde marker fast blue (1.7% wt/vol in sterile water) was injected (volume: 1–2 µl) at multiple sites along the colon. The gut was swabbed after each injection to remove seepage and prevent indiscriminate labeling before being replaced in the abdomen, which was closed by suturing.

#### *Immunohistochemistry*

Whole DRGs from mice injected with fast blue were mounted in Optimal Cutting Temperature (O.C.T.) compound (Sakura - Tissue Tek), freezed with liquid N<sub>2</sub>, and



kept at – 80 degrees. DRG slices (10 µm) were cut and mounted in slides and frozen at – 80 degrees. Abcam for IHC-Fr was the technique used: slices were fixed with 4% paraformaldehyde for 10 min at room temperature and washed three times with phosphate buffered saline (PBS) plus 0.025% Triton X-100. The nonspecific binding sites were blocked with 10% normal bovine serum albumin (BSA) for 2 hrs at room temperature then we applied the primary antibody (anti-TLR4) diluted 1% BSA in TBS (Tris Buffered Saline) at the dilution 1:500 and incubated overnight at 4 degrees. The slices were rinsed 2 times for 5 minutes with TBS. The secondary antibody diluted 1:2000 was applied to the slices and incubated for 1 hr at room temperature in dark conditions. Preparations were mounted in 50% glycerol. The images were digitally acquired with fluorescence microscope Olympus BX51.

#### *ELISA method to quantify TNF-α induced by LPS in Culture Supernatants*

Equal volumes of dispersed DRG neurons were plated onto laminin/poly-D-lysine coated coverslips in a 24-well plate containing 1 ml culture media per well; 10 µg/ml ultrapure LPS (*E. coli* O55:B5) was added and incubated at 37°C in a humidified incubator with an atmosphere of 95% O<sub>2</sub>/5% CO<sub>2</sub>. After overnight incubation, the culture supernatants were harvested and stored at -80°C for ELISA measurement of released TNF-α. Mouse TNF-α ELISA kits were obtained from R&D Systems, Minneapolis, MN. Assay of samples and standards were performed simultaneously according to the manufacturer's instruction. Briefly, polyclonal anti-mouse TNF-α antibodies were used as capturing antibodies and horseradish-

conjugated polyclonal anti-mouse TNF- $\alpha$  antibodies as the detecting antibody. Stabilized hydrogen peroxide and chromogen were added as color reagents. Optical densities of each well were determined by using a microplate reader-Titertek Multiskan Plus photometer set at 450 nm within 30 min the color reactions were stopped. All steps were performed at room temperature and samples were assayed in duplicate.

#### *Antibodies and Reagents*

The polyclonal anti-rabbit anti-NF $\kappa$ B p65 (#3034), monoclonal anti-rabbit anti-phospho-NF $\kappa$ B p65 (#3033), polyclonal anti-rabbit anti-p38 MAP kinase (#9212), polyclonal anti-rabbit anti-phospho-p38 MAP kinase (#9211), and anti-rabbit secondary antibody (#7074) were obtained from Cell signaling Technology (Danvers, MA, USA). Rabbit polyclonal anti-TLR4 antibody (ab13556) was obtained from Abcam (Cambridge, UK). The Alexa Fluor<sup>®</sup>568-conjugated goat polyclonal to mouse IgG (H&L), Anti-rabbit anti- $\beta$  actin antibody (A5316) were purchased from Sigma Aldrich, the ultrapure LPS and LPS “Standard grade” (Escherichia coli serotype 055:B5) were purchased from Sigma-Aldrich (Oakville, Ontario, Canada).

#### *Acute application experiments*

Equal volumes of dissociated neurons were plated at high density on coverslips and incubated for 22 hr of final time at 35°C. In these cultures, experiments were carried out using different concentrations of LPS or ultrapure-LPS and several

application times (5, 20, 60 and 120 minutes). After completing application time, supernatant was discarded and neurons were washed with PBS and collected with Trizol Reagent. Stock solution of LPS from *Escherichia coli* 055:B5 strain ("standard-grade"; Sigma-Aldrich, Oakville, Ontario, Canada), and ultrapure LPS from *E. coli* 0111:B4 (InvivoGen via Cedarlane, Hornby, Ontario, Canada), and 055:B5 (Sigma-Aldrich) strains were dissolved into injectable water to 5 mg/ml, aliquoted and stored at -20°C. *E. coli* NLM28 preparations were a kind donation from Dr. Nancy Martin (Queen's University). Briefly, a single bacterial colony was inoculated in 5 ml Luria-Bertani medium and incubated overnight at 37°C. One milliliter of such medium was transferred to 50 ml Luria-Bertani medium and cultured at 37°C until the bacteria reached a concentration of  $\sim 10^8$  cells/ml. The bacterial culture was spun down at 13,000 rpm for 2 min, and the pellet washed once with Luria-Bertani medium, before respinning and resuspension in the same amount of fresh Luria-Bertani medium or deionized water. Half of the preparation was sonicated (4 X 5 s pulses, being kept on ice for 10 s in between pulses). Cells and lysate were aliquoted and stored at -20°C until used at a final concentration of  $10^6$  cells/ml. All other bacterial products were acquired from InvivoGen. HBSS and F12 medium were purchased from Invitrogen (Carlsbad, CA), Poly-Dlysine from VWR (Mississauga, Ontario, Canada) and Papain was obtained from Worthington Biochemical (Lakewood, NJ). Dextran sulfate sodium salt (DSS), molecular mass 36–50 kDa, was purchased from MP Biomedicals (Solon, OH) and dissolved at 2% wt/vol in tap water. All other substances were obtained from Sigma-Aldrich.

### *LPS effects on Colonic Afferent Nerves*

Experiments were performed on colons from control and treated CD1 or C57BL/6 mice as previously described (43). Briefly, the colon was removed with attached mesentery and placed in a Sylgardlined organ chamber continually superfused with oxygenated Krebs solution (in mM: 118.4 NaCl; 24.9 NaHCO<sub>3</sub>; 1.9 CaCl<sub>2</sub>; 1.2 MgSO<sub>4</sub>·7 H<sub>2</sub>O; 1.2 KH<sub>2</sub>PO<sub>4</sub>, and 11.7 D-glucose) at a flow rate of ~6–7 ml/min and maintained at 33–34°C. Proximal and distal ends of the bowel were securely attached to an input and outlet port. The input port was connected to a perfusion syringe pump, which allowed continuous intraluminal perfusion of Krebs solution through the segments (0.2 ml/min). The mesenteric bundle was pinned out on the base of the chamber, and a mesenteric nerve was dissected out from the bundle and drawn into a glass pipette by applying suction to the pipette holder. This holder was connected to a Neurolog headstage (NL 100, Digitimer Ltd). Electrical activity was filtered (using a preamplifier NL125 with a low and a high band pass of 0.060 and 20 kHz, respectively) and then amplified (with the amplifier NL104, Digitimer Ltd). Electrical activity was digitized (at 20 kHz sampling rate) using a Micro 1401 MKII interface (Digitimer Ltd) to a PC running Spike 2 software (Cambridge Electronic Design) (Figure 11).

The preparation was stabilized for 60 min and we performed experiments in the presence of bacterial lysate, standard-grade LPS, or ultrapure LPS 30 µg/ml applying the drug into the bath for 5 min and washing it out for 30 min.

### *Chronic DSS Inflammatory Model*

C57BL/6 mice underwent three cycles of alternating 5-day periods receiving 2% DSS in drinking water and 5-day periods of normal drinking water. Mice had access to food and fluids *ad libitum*. Subcutaneous injections of 0.5 ml lactated Ringer's solution were administered daily to DSS-treated mice to avoid dehydration, and weight loss was closely monitored, to avoid unnecessary suffering, a loss of 15% was considered as the threshold for euthanasia. Following the final water cycle, mice were euthanized and their colons removed, as described above, to assess colonic afferent responses to bacterial lysate.

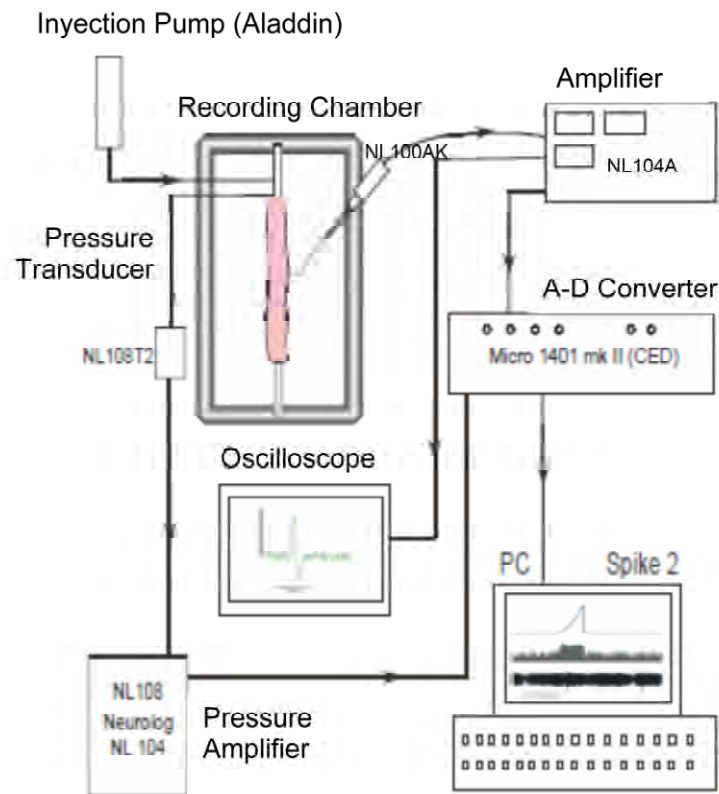


**Figure 11. Setup to record the multiunitary activity and the intestinal distension.** The mouse colon was placed in a Sylgardlined organ chamber continually superfused with oxygenated Krebs. Proximal and distal ends of the colon were firmly attached to an input and outlet ports. The input port was connected to a perfusion syringe pump (continuous intraluminal perfusion of Krebs solution). The mesenteric bundle was pinned down on the base of the chamber, and a mesenteric nerve was dissected out from the bundle and drawn into a glass pipette by applying a slight suction into the pipette holder. This holder was connected to a Neurolog headstage (NL100AK). Electrical activity was filtered and then amplified. Electrical activity was digitized (at 20 kHz sampling rate) using a Micro 1401 MKII connected to a personal computer running Spike 2 software (61).

## V. RESULTS

### *a. DRG Neurons that project to the colon show the transcript of pattern recognition receptors.*

Approximately one hundred DRG neurons were labeled with fast blue after injecting this substance into the colon wall. These neurons were isolated by laser capture microdissection technique (LCM) (43, 47) and by using RT-PCR we determined the expression of pattern recognition receptors (PPRs). Transcript for TLRs 1, 2, 3, 4, 5, 6 and 9, nucleotide binding oligomerization domain containing receptors (NOD) 1-2, and the adapter proteins MyD88, MD1 and MD2 were detected (Figure 12 is representative of 3 separate experiments).

### *b. DRG Neurons projecting to the colon show immunoreactivity for Toll-Like Receptor 4*

DRG slides, from the corresponding spinal segments T9-T13, were incubated with anti-TLR4 antibody, all slices had a large number of neurons with immunoreactivity for TLR4. Figure 14 shows an example of the 15 slices. In these same slices we were able to observe 3 neurons that were marked with fast blue, indicating that these neurons were innervating the colon wall (Figure 13). These three neurons showed also immunoreactivity for Toll-Like Receptor 4.

*c. LPS Activates NF-κB Pathway*

Incubation with 1 μg/ml LPS (*E. coli* 055:B5) or 1 μg/ml ultrapure LPS (*E. coli* 055:B5) increased the phospho Ser<sup>536</sup> p65 (NF-κB) detected (Figure 15, A and B; representative Western blot from 3 separate experiments), in dissociated DRG neurons from the corresponding spinal segments T9-T13. We observed in the panel A, from the total protein samples of neuron culture treated with 1 μg/ml ultrapure LPS that the amount of detected phospho Ser<sup>536</sup> p65 increased in a time-dependent manner. While in the panel B, phospho Ser<sup>536</sup> p65 detected from total protein samples of neuron culture treated with 1 μg/ml ultrapure LPS showed a similar increase in each time tested.

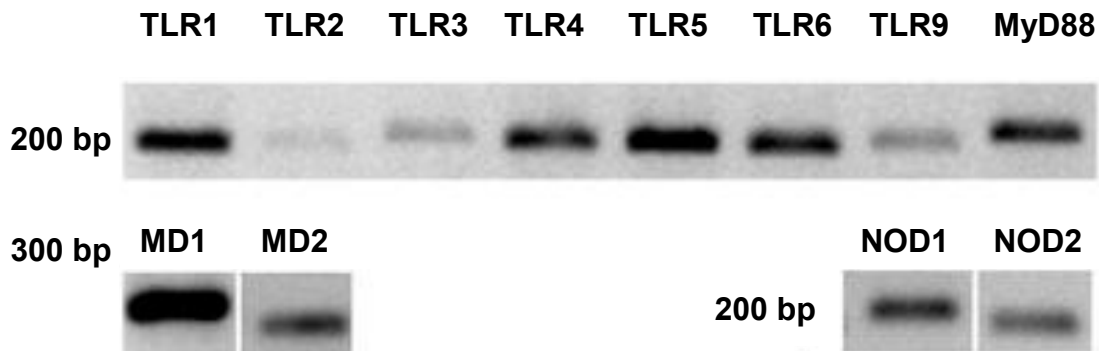


**Figure 12. Toll-like receptors (TLRs) and supplementary proteins are express in dorsal root ganglia (DRG) neurons that project to the colon.** Neurons were identified using the fast-blue labeling technique, which was injected in the colon wall 2-3 days before collecting them. These labeled neurons express diverse TLRs and other proteins involved in pathogen-associated molecular pattern signaling, as detected by RT-PCR and agarose gel electrophoresis. Results of one representative experiments out of three, are shown here.



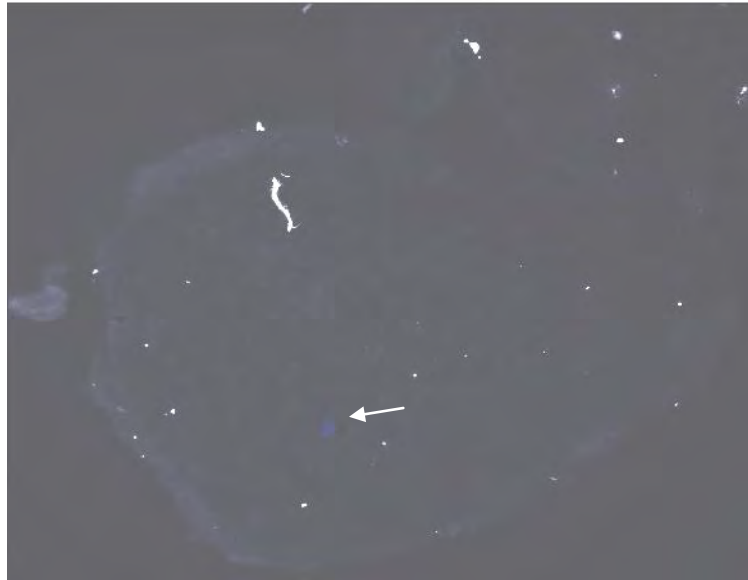


**Figure 13. Colonic Projecting DRG Neuron showing fluorescence for the retrograde marker Fast Blue.** Frozen DRG slides showing fast blue fluorescence (excited with wavelength 365 nm) were treated with Immunohistochemistry for anti-TLR4. We found three colonic projecting DRG neurons in 15 slides of different ganglia. The arrow indicates a colonic projecting DRG neuron.

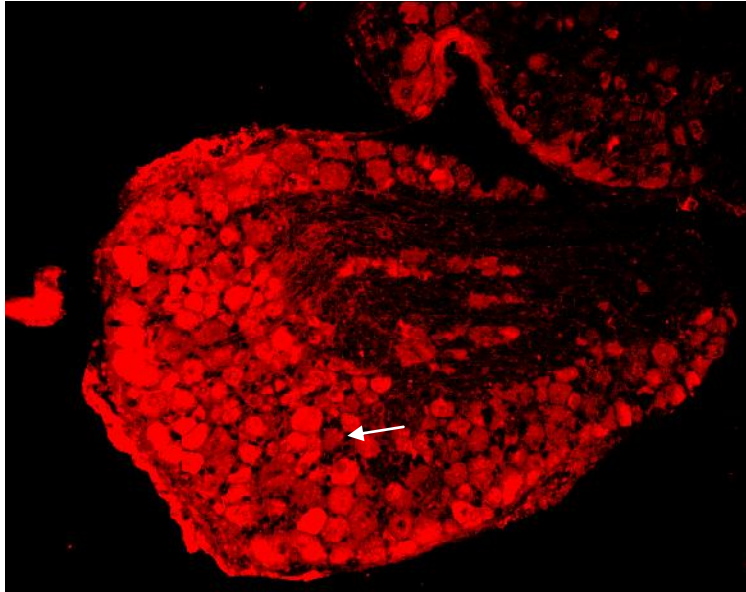


**Figure 14. Slides of mouse DRG show Immunoreactivity for TLR4.** Using Ab13556 as an antibody we look for TLR4 staining on neurons by Immunohistochemistry. Slides were fixed with paraformaldehyde and blocked with 10% BSA for 2 hrs at room temperature. Slides were incubated with primary antibody (1/500) overnight at 4 °C. Alexa Fluor<sup>®</sup>568-conjugated goat polyclonal to mouse IgG (H&L) was used as secondary antibody at a 1/2000 dilution and incubated for 1 hr at room temperature in dark conditions. The arrow indicates a colonic projecting DRG neuron showing immunoreactivity for TLR4. The images were captured with the microscope Olympus BX51 at 20X.

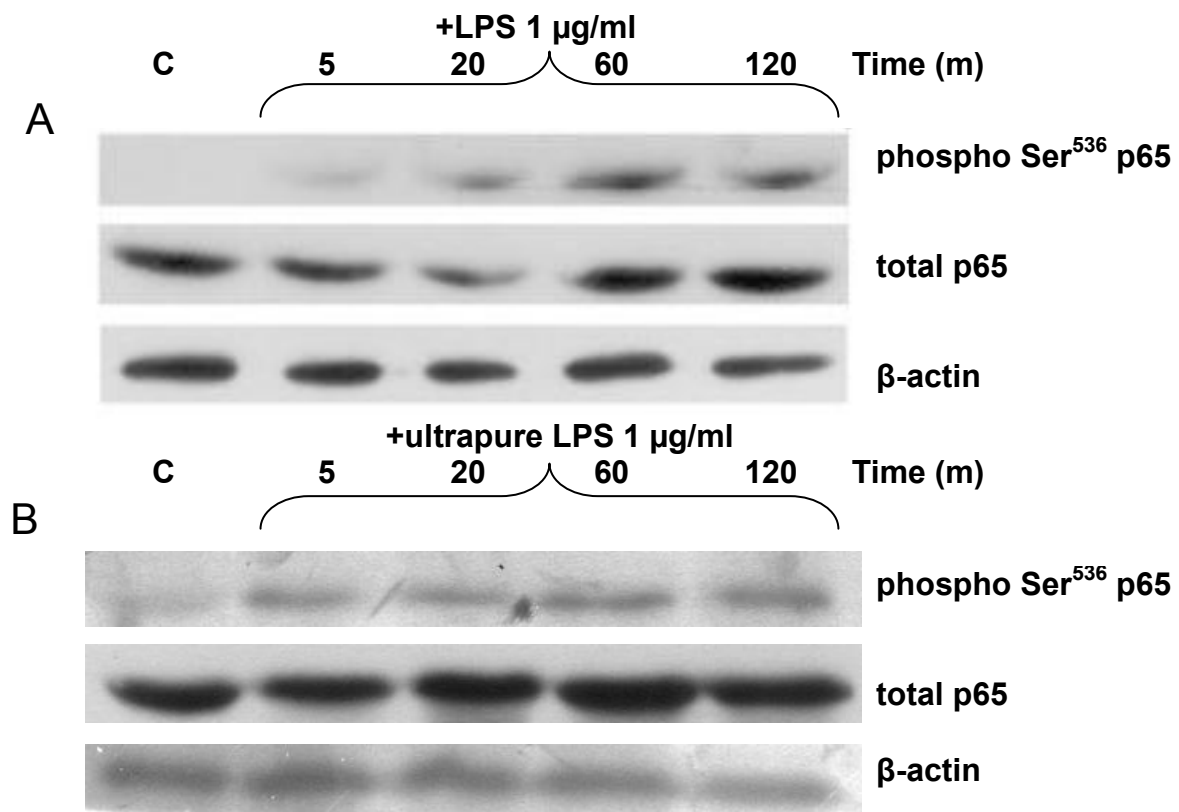


**Figure 15. NF $\kappa$ B Pathway is activated by LPS.** Western Blot of total protein samples from dissociated neurons incubated with 1  $\mu\text{g/ml}$  LPS (A) or 1 $\mu\text{g/ml}$  ultrapure LPS (B) during 0, 5, 20, 60 120 minutes. Neurons were harvested and their proteins were recovered with Trizol reagent. In each lane of SDS-PAGE (10% gels) were run 40  $\mu\text{g}$  of total protein samples and transferred onto PVDF membranes. Blotted membranes were incubated with different primary antibodies (phospho Ser<sup>536</sup> p65, total p65 and  $\beta$ -actin) and next with secondary antibody. The signal was detected by chemiluminescent and these experiments were carried out at 37  $^{\circ}\text{C}$ .

#### *d. Increased Expression of Cytokines*

We wanted to test if the activation of NF $\kappa$ B pathway was associated with an increase in the expression of cytokines in DRG neurons in culture. We examined changes in mRNA levels of TNF- $\alpha$ , IL-1 $\beta$  and IL-6 after the neurons were incubated in the presence of 1  $\mu$ g/ml ultrapure LPS (*E. coli* 055:B5; ultrapure) or 1  $\mu$ g/ml LPS (*E. coli* 0.55:B5). Expression of TNF- $\alpha$  was different between LPS and ultrapure LPS, with LPS the increase in the expression was the same among all application times, whereas the expression with ultrapure LPS was increased in a dependent-time manner (Figure 16, A and B). LPS (both, ultrapure and standard) caused an increase in transcript of IL-1 $\beta$  in the application time of 60 and 120 minutes, while in transcript of IL6 did not have an effect in the expression (Figure 16, A and B; representative of 3 different experiments).

#### *e. LPS Increase Cytokine Release*

Dissociated neurons from T9-T13 DRG were also incubated overnight with 10  $\mu$ g/ml ultrapure LPS and the levels of TNF- $\alpha$  in the medium were measured by ELISA. The incubation with LPS induced a ~20% increase in TNF- $\alpha$  ( $n=3$ ;  $P=0.013$ ) (Figure 17).

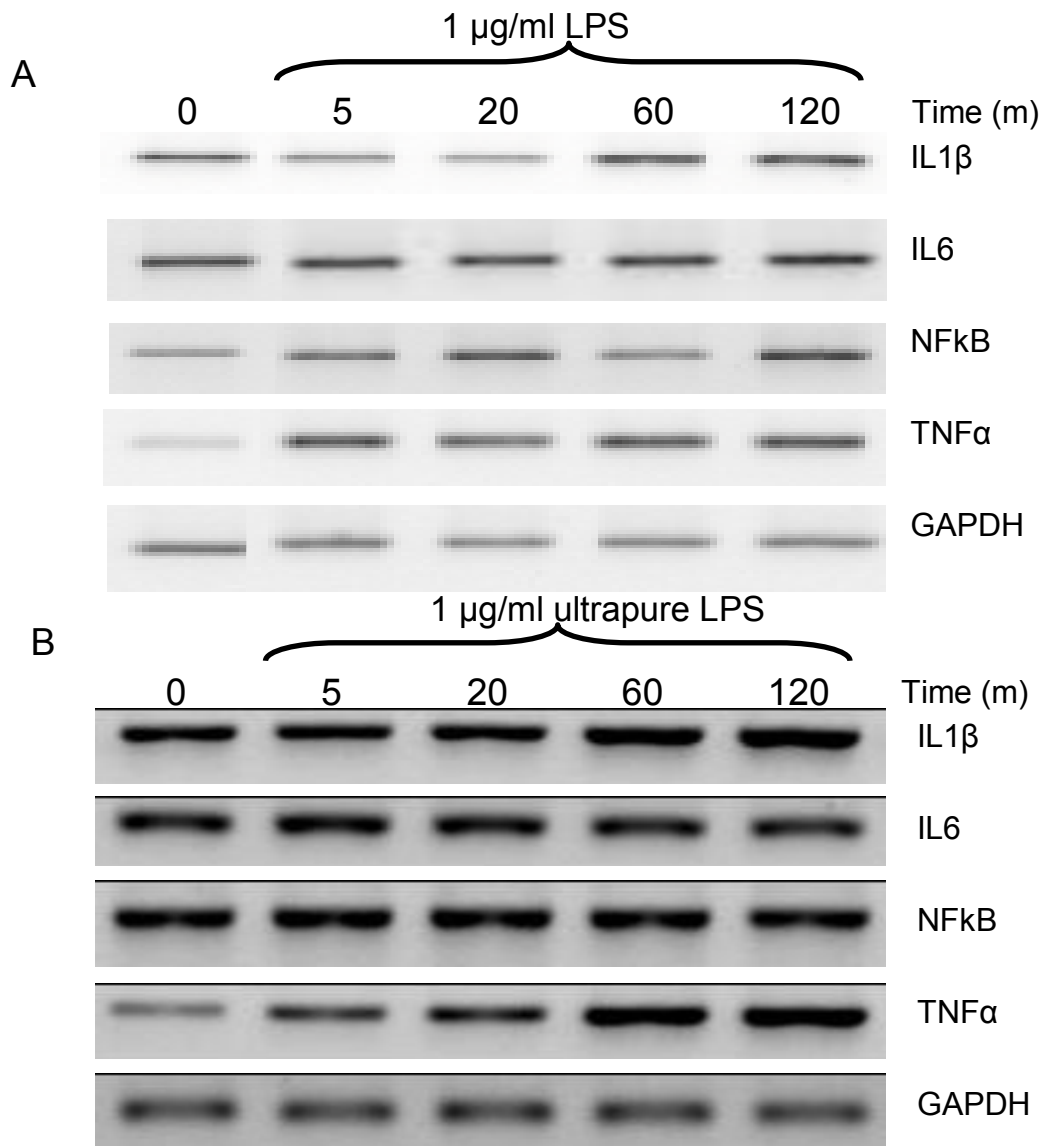


**Figure 16. LPS and ultrapure LPS increased the expression of cytokines in DRG neurons.** RT-PCR experiments show that application of LPS (A) and ultrapure LPS (B) in culture medium of dissociated DRG neurons enhanced mRNA levels of TNF- $\alpha$  and IL-1 $\beta$ . Data are from one representative experiment, out of three.

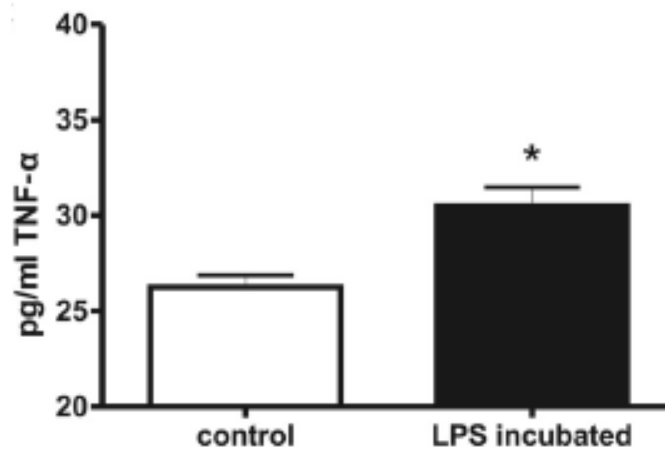


**Figure 17. LPS increase release of TNF $\alpha$ .** Overnight incubation with 10  $\mu$ g/ml ultrapure LPS significantly increased the secretion of TNF $\alpha$  by cultured DRG neurons (ELISA, P 0.013, n=3).

*f. Colonic Afferent Responses to LPS*

The afferent nerve discharge increased during application of standard grade LPS 30  $\mu$ g/ml (*E. coli* 055:B5) in multiunit afferent recordings from the mouse colon (Fig. 18 A; n=3) whereas ultrapure LPS (*E. coli* 055:B5) had no effect (Fig 18 B; n=3).

We investigated in a separate set of experiments, the impact of bacterial cell lysate over the activity of colonic afferent nerve from control and chronic DSS mice. There was a small enhance in afferent firing rate for a 5-min application of bacterial lysate to control tissues ( $0.624 \pm 0.42$  imp/s,  $n = 8$ ); nevertheless, this response was significantly larger for those tissues from chronic DSS mice ( $4.143 \pm 1.74$  imp/s,  $n = 5$ ,  $P = 0.033$ ) (Figure 19).

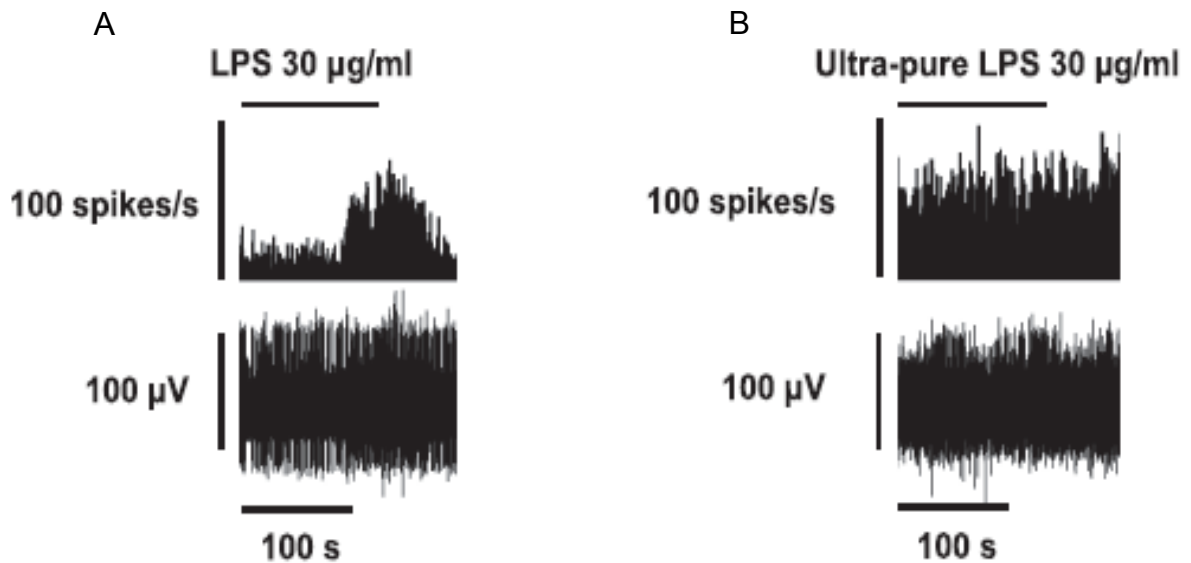


**Figure 18. Only standard-grade LPS increased colonic afferent nerve discharge.** We observed that just standard-grade LPS increased the firing frequency of in vitro mesenteric colonic multiunit nerve recordings; figure traces of the effects of standard grade LPS (left) and ultrapure LPS (right) (both 30 µg/ml from *E. coli* 055-B5). Bottom traces show raw multiunit recording; top traces show firing frequency.

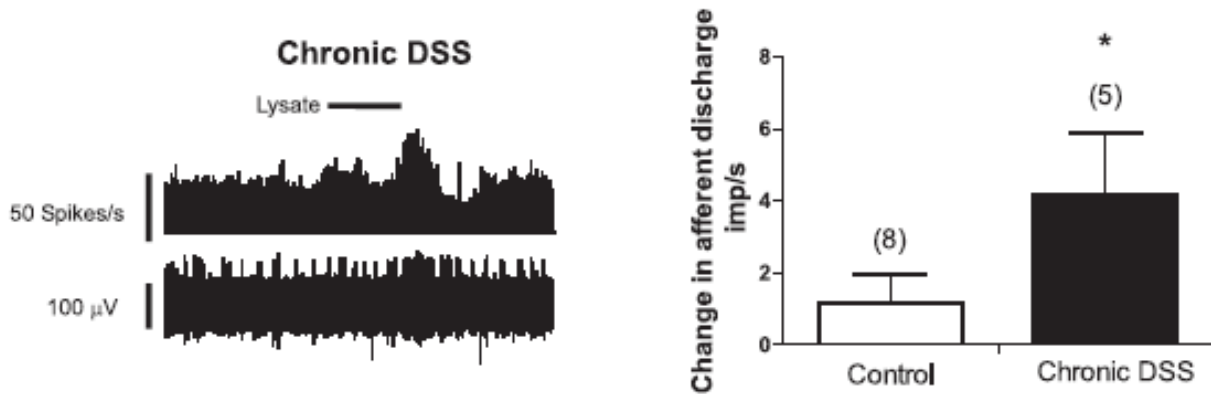


**Figure 19. An undetermined product of lysated bacteria is able of increasing colonic afferent nerve discharge.** *left*: representative traces of colonic multifiber afferent response to a bath application (5 min) of bacterial cell lysate on tissue from control or chronic DSS mice. *Top* traces show whole the nerve activity histogram; *bottom* trace is the raw whole nerve spike activity. *Right*: means  $\pm$  SE of control ( $n = 8$ ) and chronic DSS ( $n = 5$ ) experiments. Colonic afferent nerve response to the bacterial cell lysate was significantly higher on chronic DSS compared with control tissues; unpaired  $t$ -test,  $P = 0.033$ .



## VI. DISCUSSION

This study examined whether lipopolysaccharides (LPS) can directly signal to colonic DRG neurons. We identify DRG neurons with prolongations to colon using retrograde fast blue marker, and determined that these neurons express the accessory proteins and toll-like receptors that are important for identifying pathogen-associated molecular patterns (PAMPs), and that exposure to LPS of DRG neurons activates NF- $\kappa$ B signaling pathway and transcription of proinflammatory genes. This study is complemented by electrophysiological results obtained in our laboratory, which will be integrated into this discussion below.

Approximately 60% of the weight of fecal matter contained in the colon corresponds to bacteria, this is about  $10^{14}$  cfu/g stool and they are in direct contact with the colonic epithelium (26, 43). The presence of bacteria in the gut, both beneficial or pathogenic act by activating toll-like receptors, through PAMPs, causing inflammation and pain (3). Under conditions where the permeability of the intestinal epithelium is compromised, the inflammatory process may be exacerbated by TLR signaling pathway. Currently have been identified 10 TLR in human and 13 in mouse (46, 50). Ligands are known to most of these receptors except for 10, 12 and 13 (West et al., 2006), among some of these ligands we found, lipopolysaccharide activating TLR4, lipopeptide to TLR 1, 4, 6, ds RNA to TLR3, etc. (26). Other ligands known to act on TLR4 is heat shock protein 60 and 70 of bacteria and host, taxol of plant, fusion proteins of respiratory syncytial virus, etc. (19, 77).

We employed laser capture microdissection (LCM) to isolate fast blue-labeled DRG neurons (i.e., colonic neurons) and examine TLR mRNA expression. We identified transcripts for TLR 1, 2, 3, 4, 5, 6, 9, and the Md 1–2 and MyD88 adapter molecules. While in myeloid cells a functional receptor for LPS is composed of CD-14, MD-2 and TLR4, and mature B cells by MD-1 and RP105, we found a strong expression of MD-1 in DRG neurons, which involves an unusual combination of proteins to form a functional TLR4 receptor (1). Moreover, we found immunoreactivity for the receptor TLR4 in fast blue labeled DRG neurons projecting to the colon. This finding suggests that these sensory neurons have the capacity to respond to a wide array of molecular epitopes or pathogen associated molecular patterns (PAMPs) and specifically for the TLR4 ligands.

The TLR4 receptor may act on two signaling pathways, a MyD88-dependent and another independent, the dependent in turn might activate two transcription factors (65). In DRG neurons we found that the functional signaling pathway is that of NF- $\kappa$ B, where this transcription factor is released and translocated to the nucleus of the cell. Activation of NF- $\kappa$ B directs the synthesis of inflammatory cytokines such as TNF- $\alpha$ , IL-1 $\beta$ , and IL-6. We tested this possibility with the application of standard LPS and ultrapure LPS in culture dissociated DRG neurons, removing nonneuronal cells by isolating neurons via centrifugation with percoll and treating the cultures with  $\beta$ -ARAC (see MATERIALS AND METHODS).

We found evidence that TLR4 ligand ultrapure LPS activates the transcription factor NF $\kappa$ B independently of the incubation time, while with the standard ligand LPS is time dependent. In both cases, transcript of TNF- $\alpha$  and IL-1 $\beta$  are increased.

Using an ELISA protocol, we also provided direct evidence for secretion of inflammatory cytokines (TNF- $\alpha$ ) from DRG neurons incubated in culture medium with standard LPS. These findings suggest a novel landscape in which DRG neurons are directly involved in the inflammatory response mediated by PAMPs. The release of proinflammatory cytokines could have an effect on the same neuron or neighboring neurons in the DRG, which would increase the sensitivity of the axon terminals of DRG neurons in the gut or in others areas innervated by neighboring neurons.

Further studies should also explore the possibility that release of inflammatory mediators from the soma within the ganglia themselves could also enhance signaling between adjacent neurons. This could include direct neuronal signaling as well as the activation of the microglia, which in turn signal to adjacent neurons in the ganglia (60).

Other electrophysiological studies performed in our laboratory confirm our results. We have found that chronic incubation of ultrapure LPS with acutely dissociated DRG neurons for 24 h markedly increased the excitability of these neurons, consistent with the activation of TLR-mediated pathway (Figure 20).

Moreover, in the case of acute applications (i.e. minutes) of bacterial cell products has been suggested that may increase directly the excitability of DRG neurons (39, 76). We have obtained results that support this, where the application of standard LPS for 3 minutes on dissociated DRG neurons increases neuronal excitability, decreases the rheobase and increases the membrane hyperpolarization (Figure 21). These actions, however, appear to involve a number of ionic mechanisms, some of which are not TLR4 mediated and would have

competing effects on neuronal excitability. Simultaneously, standard-grade LPS induced a decrease in rheobase (no with ultrapure LPS) and increase the excitability, implying the modulation of voltage-gated Nav and/or Kv currents (11, 74).

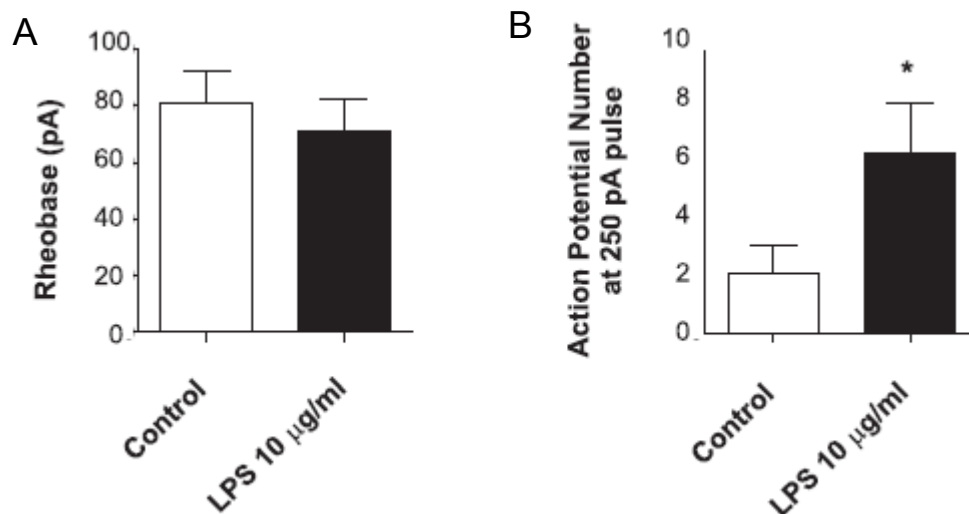


**Figure. 20. Chronic incubation with ultrapure LPS increases DRG neuronal excitability.** Current-clamp recordings of fast blue labeled colonic DRG neurons to assess neuronal excitability after 24 h incubation with 10 µg/ml ultrapure LPS. A: mean rheobase was not significantly changed after incubation with 10 µg/ml ultrapure LPS ( $P > 0.05$ ,  $n = 12$ ). B: ultrapure LPS increased the mean number of action potentials (APs) produced by a 500-ms 250 pA pulse ( $2.1 \pm 1.0$  AP and  $6.4 \pm 1.8$  AP, control and LPS incubated respectively,  $P = 0.04$ ,  $n = 12$ ). Bars represent means and lines above represent SE. \*Statistical significance,  $P \leq 0.05$ .

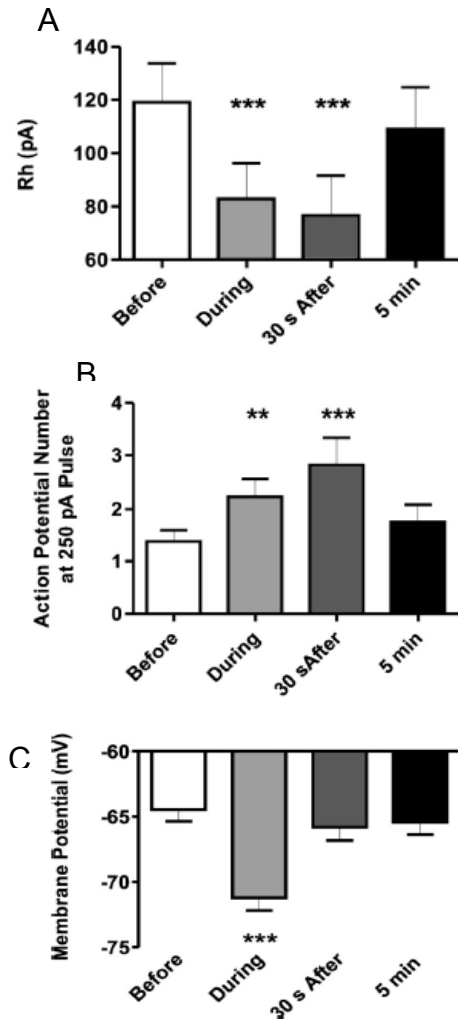


**Figure 21. Standard-grade LPS applied acutely increases DRG neuronal excitability.** Neuronal excitability of fast blue-labeled colonic DRG neurons in the presence of 30  $\mu\text{g/ml}$  standard-grade LPS. **A:** standard-grade LPS decreased mean rheobase ( $P < 0.0001$ ,  $n = 21$ ). **B:** mean number of action potentials was increased by standard-grade LPS ( $P < 0.001$  and  $< 0.0001$  for “during” and “30-s washout,” respectively,  $n = 21$ ). **C:** the mean membrane potential hyperpolarized during 30  $\mu\text{g/ml}$  standard-grade LPS ( $P < 0.0001$ ,  $n = 21$ ).

The mechanism involved in these actions is unclear, but TLR4-mediated pathway seems not to be involved in the hyperpolarization observed in electrophysiological recordings. TLR4 knockout animals was used to compare the effect of LPS on the rheobase, and the action potential discharge, and we found that the effect on rheobase appears to be lower while the action potential discharge was not observed (Figure 22).

Therefore, we examined the effect of acute treatment of ultrapure LPS against LPS standard, and we note that ultrapure LPS had no effect on the properties of the membrane of the neuron in patch-clamp recordings and similarly no excited multiunit colonic afferent nerves multiunit (Figure 18). The explanation for this difference is not very clear but may be due to the effect of other bacterial cell products in the standard-grade LPS or impurities (33, 37), such as adenosine or glutamate.

We tried to clarify whether the presence of impurities in the standard-grade LPS affect electrophysiological actions, for which we examined the effect of acute treatment of a bacterial lysate prepared from a nonpathogenic strain of *E. coli* (NLM28). We found that lysate increased action potential discharge (Figure 23). Furthermore, we found that the lysate acutely applied activated more significantly colonic afferent of inflamed bowel obtained from mice treated chronically with DSS, compared with controls (Figure 19). Whether this difference is the result of an increase in the expression of TLRs induced by inflammation (34, 64), access of the lysate to tissue altered, or another mechanism such as altered intrinsic firing threshold of the axons is unclear. Yet, these studies do argue against an exclusive role for impurities but the mechanism underlying the actions of the cell products involved remains to be determined. We examined the individual actions of membrane lipoproteins, peptidoglycan and RNA that have been reported to signal through TLRs but did not observe a change in neuronal excitability. Therefore other products appear to be involved in mediating the actions of the bacterial cell lysate on neuronal excitability.

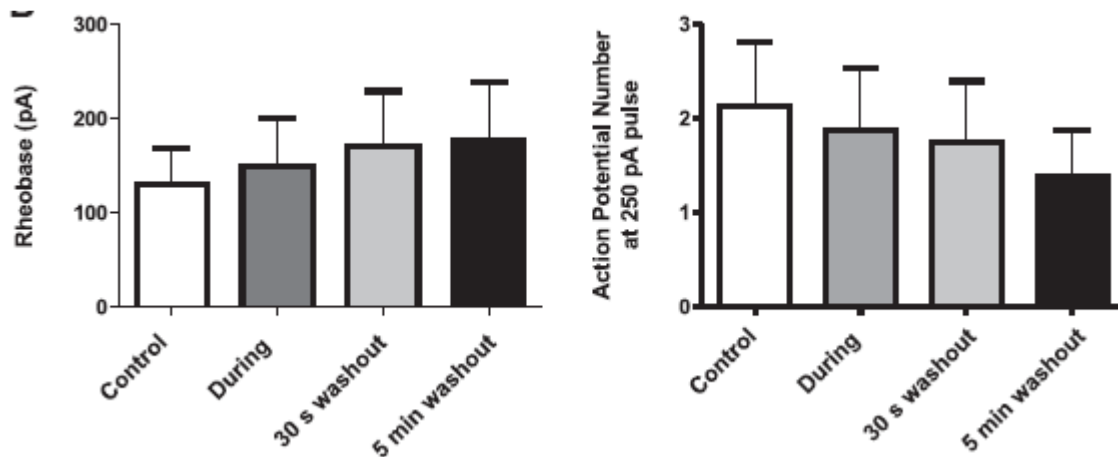


**Figure 22. Effects of standard-grade LPS on excitability are not TLR4 mediated.** 30  $\mu\text{g/ml}$  ultrapure LPS from *Escherichia coli* 055:B5 did not reproduce the effects of standard-grade LPS on rheobase or number of action potentials ( $n=5$ ), *Left*: mean rheobase before, during 30  $\mu\text{g/ml}$  standard-grade LPS, and after washing. *Right*: mean action potential number at 250 pA before, during 30  $\mu\text{g/ml}$  standard-grade LPS, and after washing.

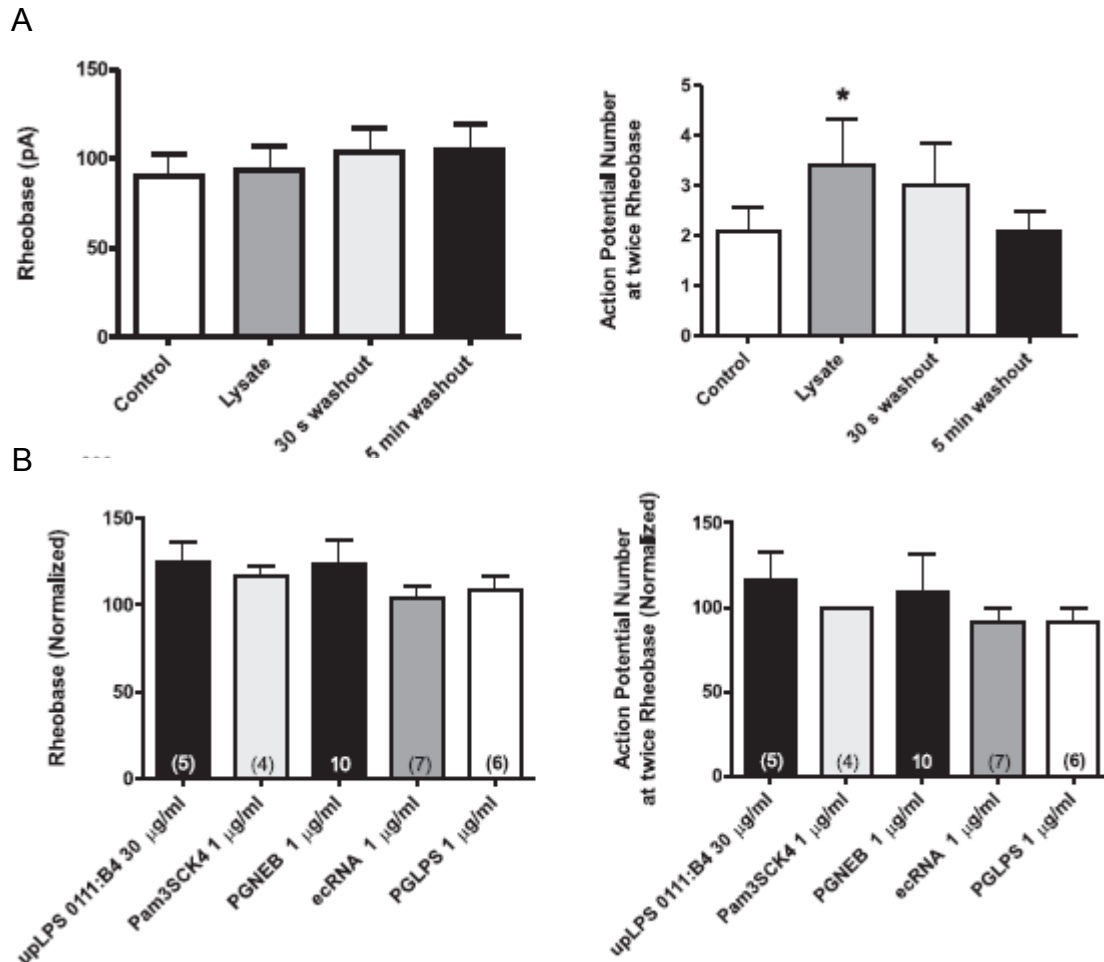


**Figure 23. An undetermined product of lysated bacteria is capable of enhancing DRG excitability and colonic afferent nerve discharge.** Current-clamp recordings of fast blue-labeled DRG neurons. *A*: summary data of the effects of lysated *E. coli* NLM28 bacteria on rheobase and action potential numbers. The lysate enhanced the number of action potentials at twice rheobase ( $P=0.02$ ,  $n=10$ ). *B*: selected bacterial products do not reproduce the effects of standard-grade LPS or lysated bacteria. Summary data of normalized rheobase (*left*) and action potential number at twice rheobase (*right*) in the presence of Pam3SCK4 (1  $\mu$ g/ml,  $n=4$ ), peptidoglycan from *E. coli* 0111:B4 strain (PGNEB; 1  $\mu$ g/ml,  $n=10$ ), *E. coli* K12 RNA complexed with LyoVec (ecRNA; 1  $\mu$ g/ml,  $n=7$ ), and *Porphyromonas gingivalis* (PGLPS; 1  $\mu$ g/ml,  $n=6$ ). Results in plots are presented as means  $\pm$  SE; \*statistical significance,  $P \leq 0.05$ .



## VII. CONCLUSION

In summary, we found that DRG neurons with projections colonic express a battery of pattern recognition receptors (PPRs), and the lipopolysaccharide present in the colon could be acting on these neurons by activating the signaling pathway of NF- $\kappa$ B. The activation of this nuclear transcription factor start the transcription of proinflammatory genes such as TNF- $\alpha$  and IL-1 $\beta$ , which could act by an autocrine or a paracrine manner, increasing the inflammatory response and sensitizing and activating the axon terminals of DRG neurons in the colon. Plus, we observed that bacterial cell products alter the intrinsic excitability of nociceptive DRG neurons and they have the potential to acutely modulate pain signaling. More research is needed about the many factors that could influence the magnitude of this effect, including the ability of bacteria to access directly to the axons of the DRG in the interstisium in conditions such as inflammatory bowel disease (IBD) in which expression of TLR can be markely increased during inflammation and of course the nature of bacterial cellular products that activate them. Furthermore, studies should ensure the purity of the products used.

## VIII. APPENDIX A

### CLONACIÓN DE RECEPTORES IONOTRÓPICOS INVOLUCRADOS EN EL PROCESO INFLAMATORIO

#### ANTECEDENTES

El dolor es una sensación que alerta a un organismo acerca de una amenaza inminente de daño tisular. El dolor inflamatorio se produce por el aumento de la excitabilidad de las fibras sensoriales periféricas nociceptivas que ocurre por la acción de mediadores inflamatorios. Estos están involucrados en la génesis, persistencia y severidad del dolor seguido del trauma, infección o daño nervioso (32). El efecto excitatorio, en turno, es un resultado de la actividad alterada de los canales iónicos dentro de las fibras sensoriales afectadas. La acción de los mediadores inflamatorios sobre las neuronas sensoriales está determinado por sus receptores específicos: (1) Receptores acoplados a proteínas G; (2) Receptores con actividad de cinasa de tirosina y (3) Receptores ionotrópicos.

Cuando existe daño de tejido o inflamación, el ATP puede ser liberado de células dañadas o las neuronas sensoriales pueden liberar ATP bajo estimulación nociva, activando a los receptores P2X. La activación de estos receptores P2X inicia el flujo de  $\text{Ca}^{2+}$  a través de los receptores canal P2X resultando en la despolarización y el flujo secundario de  $\text{Ca}^{2+}$  a través de canales de  $\text{Ca}^{2+}$  dependientes de voltaje. Ambas acciones, tanto la despolarización aguda como la elevación del  $\text{Ca}^{2+}$  citosólico ejercen un efecto excitatorio y proalgésico.

La familia de receptores P2X consta de siete subunidades identificadas (P2X<sub>1-7</sub>) hasta la fecha, las cuales se agrupan como trímeros para formar un receptor funcional. Los receptores pueden ser homoméricos si están formados por subunidades iguales y heteroméricos si las subunidades son diferentes (25). Existen reportes donde involucran la activación de los canales P2X<sub>2</sub>, P2X<sub>3</sub> y P2X<sub>2/3</sub> en el desarrollo de la hiperalgesia inflamatoria en neuronas de ganglios autonómicos y sensoriales (18). Se ha sugerido que la presencia del receptor P2X<sub>3</sub> es suficiente para la respuesta aguda nociceptiva a ATP, mientras que el receptor P2X<sub>2</sub> y P2X<sub>2/3</sub> contribuirían en la fase tardía de la respuesta y que pudieran estar involucrados en la sensibilización central (16).

Por otra parte, otro objetivo de esta investigación son los receptores 5HT, los cuales son canales iónicos activados por ligandos, los cuales han sido localizados dentro de los ganglios de la raíz dorsal y terminales de fibras C y fibras aferentes nociceptivas no C. Dentro de los GRD y periféricamente, los antagonistas del receptor 5HT<sub>3</sub> actúan en sitios del 5HT<sub>3</sub> sobre fibras C y no C asociadas a inflamación para producir efectos antinociceptivos por la disminución de la liberación de sustancia P (y/o otros mediadores de inflamación neurogénica) inducida por 5HT (30).

Estamos interesados en clonar el cDNA con el ORF completo de dos receptores que se sabe que juegan papeles importantes en la señalización del proceso inflamatorio, el 5HT<sub>3A</sub> y el P2X<sub>5</sub>. Sabemos que en algunos casos se han reportado variantes de splicing alternativo de receptores que al ensamblarse en membrana como homómeros o heterómeros les confiere cualidades

farmacológicas o electrofisiológicas diferentes a las del receptor formado con la variante completa (62, 73).

Debido a que no existen reportes de splicing alternativo para la subunidad del receptor P2X5 ni en ratón ni en cobayo, y que se han reportado para otras subunidades variantes de splicing funcionales y con propiedades diferentes a las de la variante completa, decidimos caracterizar farmacológica y electrofisiológicamente las variantes de splicing de la subunidad P2X5 de ratón y cobayo que logremos aislar. En el caso del 5HT3 de cobayo, se han reportado dos variantes de splicing, que difieren en 18 pb entre el transmembranal 3 y el 4, y que según un estudio previo no les confiere diferencias entre sus propiedades farmacológicas (52). Sin embargo, la clonación de ambos receptores nos va a permitir realizar diferentes combinaciones de expresión de diferentes subunidades clonadas. Para esto fue necesario obtener por PCR con oligos específicos las variantes de P2X5 en ratón y cobayo y del 5HT3 de cobayo. Estas variantes se clonarán en el vector pcDNA3.1+ y a futuro se expresarán en ovocitos de *Xenopus laevis* para caracterizarlas farmacológica y electrofisiológicamente.

## MATERIALES Y MÉTODOS

### *Secuencia genómica y del cDNA de los receptores P2X5 y 5HT3A*

Las secuencias genómica y de cDNA que codifican para los receptores P2X5 y 5HT3A de ratón y cobayo fueron obtenidas de NCBI (<http://www.ncbi.nlm.nih.gov>) y Ensembl database (<http://www.ensembl.org>) respectivamente. La estructura exon-intrón del gen del receptor P2X5 de cobayo fue derivada de un alineamiento de secuencias de cDNA/genómico.

### *Clonación del receptor P2X5 y 5HT3A*

Tejido extraído de cerebro, timo e yeyuno proximal fue triturado en un mortero estéril con nitrógeno líquido. El kit de aislamiento de RNA RNAqueous (Life Technologies, Texas, USA) fue usado para obtener el RNA total siguiendo los pasos del protocolo del fabricante. La primera cadena de cDNA fue sintetizada usando la transcriptasa reversa Superscript II (Life Technologies, Texas, USA) en la presencia de oligo dT por 1.5 h a 42 °C. La PCR fue realizada utilizando oligos específicos para P2X5 de ratón y cobayo y para 5HT3A de cobayo, los cuales fueron diseñados en las regiones UTR 5' y 3' para poder amplificar la secuencia codificadora completa: P2X5 cobayo F1: GGCTGAGCTGGCAGCA, R1: TCGCGCAGGCATGAGGAT; P2X5 ratón F1: AGAGTGCTCGGTTGGCTG, R1: GGCCAGACATCTTTGAATC; 5HT3A cobayo F1: ATTCTCTGGAGCTCACCCCT, R1: GACCTGGCATTGAACACA. La reacción de PCR fue hecha usando la DNA polimerasa Taq Platinum (Life Technologies, Texas, USA), las condiciones fueron las siguientes: desnaturalización inicial por 5 min a 94 °C, después 40 ciclos de

desnaturalización por 20 s a 94 °C, alineamiento por 20 s a 60 °C, y extensión por 1 min 45 s a 72 °C; la extensión final fue de 5 min a 72 °C. En todas los PCR realizados se utilizó la técnica de hot start, la cual consiste en agregar la enzima DNA polimerasa 2 min después de empezada la desnaturalización inicial. Los productos de PCR fueron analizados por electroforesis en geles de agarosa al 0.8% teñidos con 1 µg/ml de bromuro de etidio. Las imágenes fueron obtenidas con Gel-Doc 2000 Gel Documentation System (Bio-Rad). Los productos fueron clonados en el vector pGEM-T Easy (Promega, Wisconsin, USA), secuenciados y subclonados en el vector pCDNA3+.

## RESULTADOS

### *P2X5 de intestino de ratón*

En la figura A1 podemos observar que el P2X5 de ratón fue encontrado en el control positivo (cerebro) que fue utilizado. Las condiciones del PCR fueron: 55 °C de temperatura de alineamiento, utilizando *hot start* y 40 ciclos de amplificación. En el caso de P2X5 en intestino con esas mismas condiciones visualizamos una banda muy débil pero del tamaño esperado. Los productos de estos PCR fueron utilizados para la clonación en pGEM T-Easy y enviados a secuenciar.

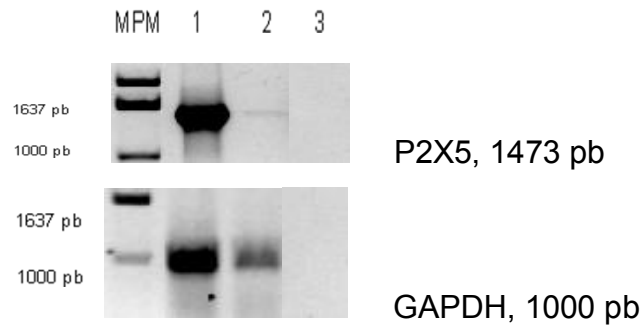


**Figura A1. P2X5 en intestino de ratón.** En la imagen superior observamos los productos de un PCR de 40 ciclos utilizando como templado cDNA de cerebro e intestino y en la inferior el de GAPDH como control. El marcador de peso molecular (MPM) utilizado fue 1 Kb de Invitrogen y los carriles corresponden a: 1- cerebro, 2- intestino y 3- control negativo. Los productos de PCR fueron corridos en geles de agarosa al 0.8% y fueron teñidos con bromuro de etidio.

Los plásmidos fueron enviados a secuenciar (McLab, California, E.U.) y dos de las secuencias dieron positivo para P2X5 con una similitud de 99%. Una de ellas retiene una secuencia de 267 pb (Figura A2.).

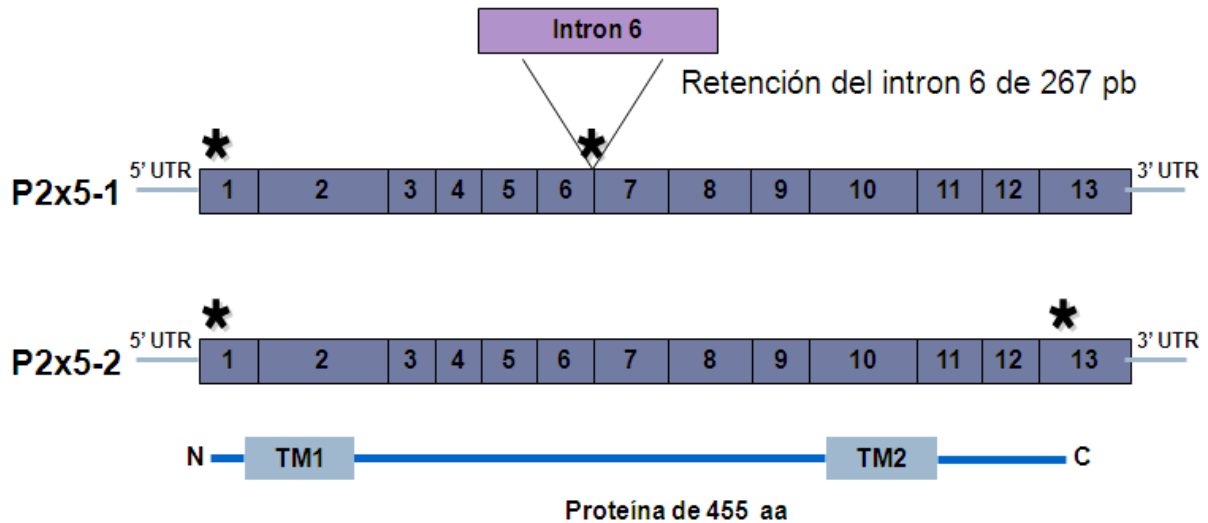


**Figura A2. Exones de P2X5 de ratón.** La variante 1 retuvo el intrón 6-7 de 267 pb y la variante 2 es la variante completa de P2X5 de ratón reportada en el NCBI con el número de acceso NM\_033321.3.

El segmento de 267 pb que retiene la variante 1 fue hibridada contra el genoma de ratón y la secuencia es 100% idéntica al intrón 6-7 (Figura A2). Con la seguridad de que teníamos dos variantes de P2X5 de intestino de ratón, las clonamos en el vector de expresión heteróloga pcDNA3.1+, y con ambos fragmentos en sentido, se linearizaron y purificaron para sintetizar RNAm invitro, que será inyectado en ovocitos de *Xenopus Laevis*.

#### *P2X5 de intestino de cobayo*

El cDNA de P2X5 de cobayo no ha sido publicado completo, por lo que se tomó en cuenta el genómico de cobayo para realizar los oligos externos para recuperar el cDNA que incluyera todo el ORF. Se compararon las 1100 pb que se conocen del cDNA del P2X5 de cobayo contra el cDNA completo del P2X5 de ratón. La similitud fue del 82%, por lo que se hibridaron las últimas 200 pb del



cDNA de P2X5 de ratón contra el genoma de cobayo (una vez localizado donde se encontraba ubicado el gen de P2X5 en *Ensemble*) y localizada la zona probable del final del ORF del P2X5 de cobayo se diseñaron oligos después de la secuencia alineada. El tamaño obtenido del fragmento de cDNA completo fue de 1479 pb.

Los oligos se probaron contra cDNA de intestino de cobayo, y de cerebro como control positivo. En la figura A3 podemos observar que el P2X5 de cobayo fue encontrado en el control positivo (cerebro) que fue utilizado y también en el intestino. El producto del PCR de intestino fue utilizado para clonarlo en pGEM T-Easy.

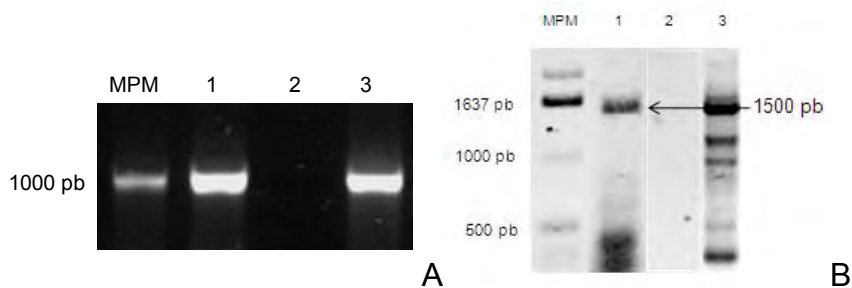


**Figura A3. P2X5 en intestino de cobayo.** A. PCR de 30 ciclos del gen GAPDH, la banda esperada es de 1000 pb. B. PCR de 40 ciclos del gen P2X5, la banda obtenida corresponde al tamaño esperado. En ambas figuras de geles el carril 1 corresponde a intestino, el 2 es el control negativo y el 3 es el de cerebro (control positivo). El marcador de peso molecular (MPM) utilizado fue 1 Kb de Invitrogen. Los productos de PCR fueron corridos en geles de agarosa al 0.8% y fueron teñidos con bromuro de etidio.

Se enviaron a secuenciación 2 plásmidos que contenían insertos con la restricción enzimática esperada. El secuencia del P2X5 de la clona 7 (Figura A3) concuerda con la isoforma 2 (completa) del P2X5 de ratón, tienen una homología

del 70%. El plásmido 2 pierde el exón 2, lo que introduce un codón de paro temprano a los 52 aa (Figura A3).

```

10      20      30      40      50      60      70      80      90
ggctgagctggcagcATGgggcaggcgggctggaaggggcttctccagtcagcgttcgactataagacagaaaagtatgtgatcgccaag 90
aacaagaaggtcgggctgctctaccgactactgcagcttaccatcgtgctgtacctgatcgtatgggtgttcggtgataaagaagggttat 180
caagacactgacacctccctgcagagtgcctgtggtcaccaaagtcaagggcgtggcctacaccaacacctcagagctgggggagcgtctc 270
tgggacgtcgcagactacgtcatccccccaggagataatgtcttcttbtgtgatcactaacctgatcgtgaccgccaaccagcgcgag 360
agcacctgtgctgagcgtgaaggcattcctgatggcatgtgttctgaggaccacgactgccctgctggggagcctgttagagctggaat 450
ggagtgaagactggccgctgtctgcgggtggggaactcgaccaggggacacctgtgagatctttgcctggtgcccagtgagacacagtcc 540
aggccagggaagccactcctgagggagcgtgaagacttcaccattttcataaagaactataattcgtttcccaagtcaatttctccaag 630
gccaatgtactagagacaaagagcaaagattttctgaaatcctgtcgctttggcccaacaatcactatgtcccattctccggctgggg 720
tccgtggtccagtgggcagggagcagcttcaggacattgccctggagggagggtgtgataggaattcacatcgagtggaactgcgacctc 810
gacagagctgcctctgagtgccatccgcgctattattttaaccgtctggacgacaaacatgtaaaatctgttcttctgggtacaactc 900
aggtttgccagataactaccgagactcagccgggtggaattccgcaacctgatgaaagcctatgggatccgcattgatgttatagttaat 990
ggaaaggcaggggaagttcagcatcgttcccacagtcacatcaatgtgggctccggggtggcgctcatgggtgctggggcttctctgtgac 1080
ctggtactcatctacatcatcaaaaagagggagtttaccgtagcaaaaagtacgaggaagtgaggggcccagagggggcggtcaggag 1170
gctgaggccaagggcgtggagcagggccagacggaggaggagcagcaggagggggagaggcaggaggagcagcctcagacctgccgag 1260
agcagcagctggaaggggaaacggcagcgtgtgcgggaagctgcctccctcccgccagaccagcgccttaaagcatgccaagggcaatgta 1350
cagcaactgcagagctctgcagacagtgaggacgTAGccaaggctgttgccgagagcaggatttgaagatcttggccagcacagctctgc 1440
agctctgaactgggaagatgcatcctcatgcctgcgcga 1479

```

**Figura A4. Secuencia del cDNA del receptor P2X5.** El cDNA fue aislado de RNAm intestinal de quinea pig. El cDNA aislado tiene un longitud de 1479 bp. Las líneas naranjas indican la secuencia de los oligos y la letra mayúscula el comienzo del codón de inicio y de paro.

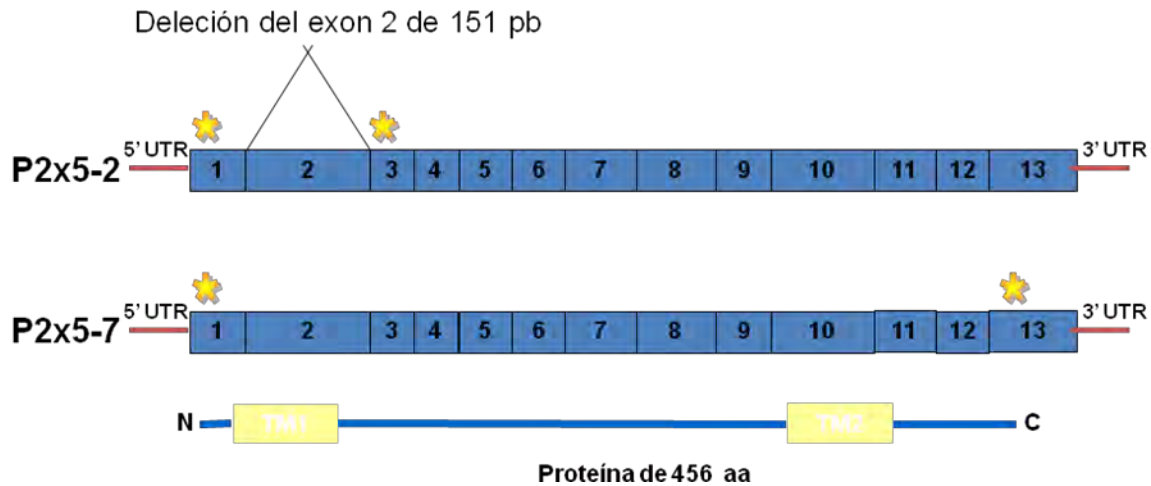


**Figura A5. Exones del P2X5 de cobayo.** La variante del plásmido 2 (que será conocida como variante 2) tiene deletado el exón 2 de 151 pb y la variante del plásmido 7 (que será conocida como variante 1) es la secuencia canónica de la subunidad P2X5 de intestino de cobayo que aún no ha sido reportada.

Las variantes se clonaron en el vector de expresión heteróloga pcDNA 3.1+ y se linearizaron para sintetizar el cRNA.

El análisis del alineamiento de las secuencias del receptor P2X5 de cobayo y de ratón (Figura A6) nos muestra que la secuencia 7 de cobayo y la 15 de ratón conservan todos los residuos de aminoácidos importantes para que la subunidad del receptor P2X5 forme un canal funcional al ensamblarse en membrana.

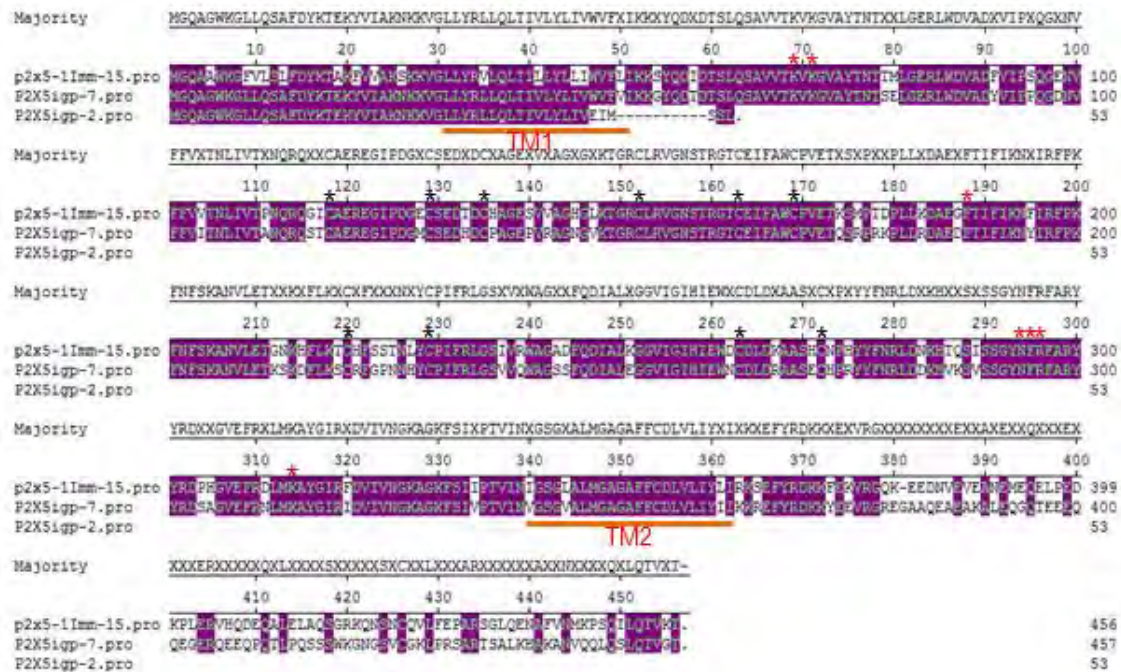


**Figura A6. Alineamiento de la secuencia de aminoácidos (aa) del receptor P2X5 de ratón y cobayo.** Las secuencias 7 y 2, son dos variantes aisladas de cobayo y la 15 de intestino de ratón. En el alineamiento: las cajas moradas y las letras encima de los residuos de aa muestran las zonas consenso. Las líneas naranja identifican los dominios transmembranales (TM1 y TM2). Las estrellas negras (118, 129, 135, 152, 163, 169, 220, 229, 263 y 272) corresponden a cada una de las diez cisteínas conservadas que son importantes para la formación de los puentes disulfuro. Las estrellas rojas (69, 71, 188, 294-296 y 314) son residuos de aminoácidos identificados por estar involucrados en los sitios de unión al ATP.

Obtuvimos la organización y el tamaño de los exones e intrones del gen del receptor *p2x5* (Figura A7). La secuencia genómica la obtuvimos de la página *Ensemble* y la alineamos contra la secuencia del P2X5 que aislamos.

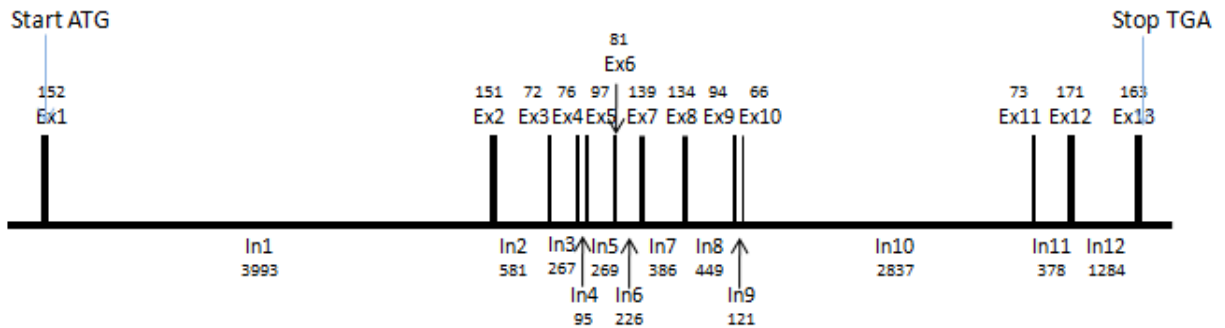


**Figura A7. Representación esquemática del gen *P2X5* de cobayo.** Las barras verticales negras representan los exones (Ex) que están distribuidos a lo largo de 12 kilobases. Los números arriba de los exones y abajo de los intrones (In) indican el largo en pares de bases. Los codones de inicio y paro se muestran con la secuencia del codon.

#### *5HT3A de intestino de cobayo*

Han sido reportadas dos variantes del 5HT3A de cobayo, con una diferencia de 6 aminoácidos entre el dominio transmembranal 3 y el 4. Con los oligos que se diseñaron para poder recuperar estas variantes, obtuvimos un fragmento de 1675 (Figura A8).

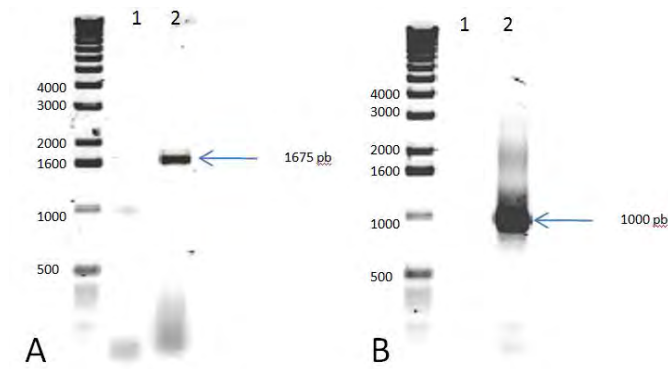


**Figura A8. 5HT3A en intestino de cobayo.** A. PCR de 35 ciclos del gen 5HT3A, la banda esperada es de 1675 pb. B. PCR de 35 ciclos del gen GAPDH, la banda obtenida corresponde al tamaño esperado. En ambas figuras de geles el carril 1 corresponde al control negativo y el 2 es de cDNA de intestino. El marcador de peso molecular (MPM) utilizado fue 1 Kb de Invitrogen. Los productos de PCR fueron corridos en geles de agarosa al 0.8% y fueron teñidos con bromuro de etidio.

Fue posible recuperar ambas variantes del 5HT3A de cobayo (Figura A9), las cuales pudimos identificar mediante secuenciación. Ambas fueron subclonadas en el vector de expresión heteróloga pcDNA3.1+.

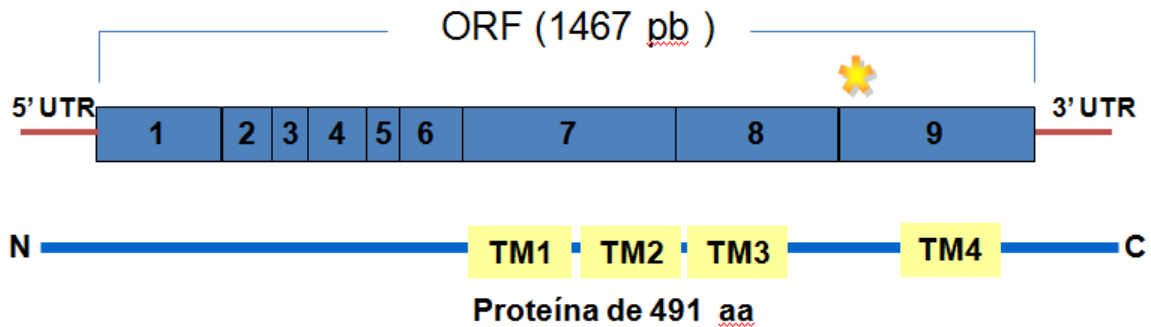


**Figura A9. Organización del gen que codifica para el 5HT3A de cobayo.** En la parte superior se muestra un esquema representativo de la organización del gen. Las cajas azules representan los exones, las líneas verticales negras representan la posición de los intrones y el asterisco señala la pérdida de 6 codones en el exón 9 generando la subunidad 5HT<sub>3AS</sub> por *splicing* alternativo. En la parte inferior se muestra el esquema representativo de la estructura de la subunidad.

Ambos plásmidos se linearizaron y purificaron para sintetizar RNAm invitro, que será inyectado en ovocitos de *Xenopus Laevis*, para caracterizar ambas variantes.

## **DISCUSIÓN Y CONCLUSIONES.**

Hemos logrado aislar exitosamente dos variantes de la subunidad de P2X5 de intestino de ratón, una de ellas la secuencia canónica reportada en NCBI y otra que retiene el intrón 6, lo que genera un codón de paro prematuro que produce una proteína trunca de 205 aa.

A su vez, de cobayo hemos aislado también 2 variantes, ninguna de las cuales ha sido reportada. Una de ellas corresponde a la secuencia canónica, ya que su arreglo genómico de 13 exones y 12 intrones, es igual al de otros P2X5 ortólogos analizados. La otra variante (clona 2) presenta una delección del segundo exón, ocasionando un codón de paro prematuro en la síntesis de la proteína, y generando una proteína de 51 aa, que no incluye los dominios transmembranales ni el asa extracelular, por lo que no formaría canales funcionales. Sin embargo, la secuencia canónica que aislamos presenta todos los residuos de aminoácidos importantes para un correcto plegamiento de la proteína y los que se sabe que están involucrados en el sitio de unión al ATP.

Lankewicz aisló y caracterizó dos variantes de la subunidad 5HT3A de cobayo y encontró una diferencia de 6 residuos de aa entre ellas (52), nosotros aislamos con éxito las secuencias de ambas variantes y las clonamos para a futuro caracterizarlas, incluyendo la posible formación de heterómeros, ya sea entre estas dos variantes o con otros 5HT3.

Todas las secuencias aisladas de los diferentes receptores, han sido corroboradas y clonadas en el vector de expresión heteróloga pcDNA3+.

## IX. REFERENCES

1. **Acosta C and Davies A.** Bacterial lipopolysaccharide regulates nociceptin expression in sensory neurons. *J Neurosci Res* 86: 1077-1086, 2008.
2. **Almeida TF, Roizenblatt S, and Tufik S.** Afferent pain pathways: a neuroanatomical review. *Brain Res* 1000: 40-56, 2004.
3. **Amaral FA, Sachs D, Costa VV, Fagundes CT, Cisalpino D, Cunha TM, Ferreira SH, Cunha FQ, Silva TA, Nicoli JR, Vieira LQ, Souza DG, and Teixeira MM.** Commensal microbiota is fundamental for the development of inflammatory pain. *Proc Natl Acad Sci U S A* 105: 2193-2197, 2008.
4. **Andoh A, Yagi Y, Shioya M, Nishida A, Tsujikawa T, and Fujiyama Y.** Mucosal cytokine network in inflammatory bowel disease. *World J Gastroenterol* 14: 5154-5161, 2008.
5. **Arciszewski MB, Sand E, and Ekblad E.** Vasoactive intestinal peptide rescues cultured rat myenteric neurons from lipopolysaccharide induced cell death. *Regul Pept* 146: 218-223, 2008.
6. **Bamias G, Nyce MR, De La Rue SA, and Cominelli F.** New concepts in the pathophysiology of inflammatory bowel disease. *Ann Intern Med* 143: 895-904, 2005.
7. **Barajon I, Serrao G, Arnaboldi F, Opizzi E, Ripamonti G, Balsari A, and Rumio C.** Toll-like receptors 3, 4, and 7 are expressed in the enteric nervous system and dorsal root ganglia. *J Histochem Cytochem* 57: 1013-1023, 2009.
8. **Bennett G.** *Neuropathic pain*. Edinburgh, UK: Churchill Livingstone, 1994.
9. **Beutler B.** Inferences, questions and possibilities in Toll-like receptor signalling. *Nature* 430: 257-263, 2004.
10. **Beyak MJ, Ramji N, Krol KM, Kawaja MD, and Vanner SJ.** Two TTX-resistant Na<sup>+</sup> currents in mouse colonic dorsal root ganglia neurons and their role in colitis-induced hyperexcitability. *Am J Physiol Gastrointest Liver Physiol* 287: G845-855, 2004.
11. **Beyak MJ and Vanner S.** Inflammation-induced hyperexcitability of nociceptive gastrointestinal DRG neurones: the role of voltage-gated ion channels. *Neurogastroenterol Motil* 17: 175-186, 2005.
12. **Birtwhistle RV.** Irritable bowel syndrome: are complementary and alternative medicine treatments useful? *Can Fam Physician* 55: 126-127, 128-129, 2009.



13. **Botos I, Segal DM, and Davies DR.** The structural biology of Toll-like receptors. *Structure* 19: 447-459, 2011.
14. **Brooks J and Tracey I.** From nociception to pain perception: imaging the spinal and supraspinal pathways. *J Anat* 207: 19-33, 2005.
15. **Cario E.** Toll-like receptors in inflammatory bowel diseases: a decade later. *Inflamm Bowel Dis* 16: 1583-1597, 2010.
16. **Cockayne DA, Dunn PM, Zhong Y, Rong W, Hamilton SG, Knight GE, Ruan HZ, Ma B, Yip P, Nunn P, McMahon SB, Burnstock G, and Ford AP.** P2X2 knockout mice and P2X2/P2X3 double knockout mice reveal a role for the P2X2 receptor subunit in mediating multiple sensory effects of ATP. *J Physiol* 567: 621-639, 2005.
17. **Córdova-Pluma V, Ibarrola-Calleja J, Hegewisch Orozco M, Domenzain P, Vargas-González M, de la Torre-Sánchez M, Castillo-González F, Maldonado-Vásquez M, Cornejo-López G, León-Merino G, Alemán-Ortiz G, Díaz-Green E, Rodríguez Weber F, Escarela-Serrano M, Cabrera-Jardines R, Orzechowsky Rayo A, Akaki-Blancas J, Betancourt-García J, de la Garza V, and Burgos A.** Frecuencia de síndrome de intestino irritable en la consulta de medicina interna y cirugía general en tres centros de atención médica de la Ciudad de México. *Med Int Mex* 24: 120-124, 2008.
18. **Dai Y, Fukuoka T, Wang H, Yamanaka H, Obata K, Tokunaga A, and Noguchi K.** Contribution of sensitized P2X receptors in inflamed tissue to the mechanical hypersensitivity revealed by phosphorylated ERK in DRG neurons. *Pain* 108: 258-266, 2004.
19. **Dalpke A and Heeg K.** Signal integration following Toll-like receptor triggering. *Crit Rev Immunol* 22: 217-250, 2002.
20. **De Giorgio R, Barbara G, Stanghellini V, Cremon C, Salvioli B, De Ponti F, and Corinaldesi R.** Diagnosis and therapy of irritable bowel syndrome. *Aliment Pharmacol Ther* 20 Suppl 2: 10-22, 2004.
21. **de Jonge WJ and Greaves DR.** Immune modulation in gastrointestinal disorders: new opportunities for therapeutic peptides? *Expert Rev Gastroenterol Hepatol* 2: 741-748, 2008.
22. **Diogenes A, Ferraz CC, Akopian AN, Henry MA, and Hargreaves KM.** LPS sensitizes TRPV1 via activation of TLR4 in trigeminal sensory neurons. *J Dent Res* 90: 759-764, 2011.
23. **Djoughri L, Bleazard L, and Lawson SN.** Association of somatic action potential shape with sensory receptive properties in guinea-pig dorsal root ganglion neurones. *J Physiol* 513 ( Pt 3): 857-872, 1998.

24. **Drossman DA, Camilleri M, Mayer EA, and Whitehead WE.** AGA technical review on irritable bowel syndrome. *Gastroenterology* 123: 2108-2131, 2002.
25. **Erb L, Liao Z, Seye CI, and Weisman GA.** P2 receptors: intracellular signaling. *Pflugers Arch* 452: 552-562, 2006.
26. **Fukata M and Abreu MT.** TLR4 signalling in the intestine in health and disease. *Biochem Soc Trans* 35: 1473-1478, 2007.
27. **Gay NJ and Gangloff M.** Structure and function of Toll receptors and their ligands. *Annu Rev Biochem* 76: 141-165, 2007.
28. **Gerold G, Zychlinsky A, and de Diego JL.** What is the role of Toll-like receptors in bacterial infections? *Semin Immunol* 19: 41-47, 2007.
29. **Gilmore TD.** Introduction to NF-kappaB: players, pathways, perspectives. *Oncogene* 25: 6680-6684, 2006.
30. **Giordano J and Schultea T.** Serotonin 5-HT(3) receptor mediation of pain and anti-nociception: implications for clinical therapeutics. *Pain Physician* 7: 141-147, 2004.
31. **Gribar SC, Anand RJ, Sodhi CP, and Hackam DJ.** The role of epithelial Toll-like receptor signaling in the pathogenesis of intestinal inflammation. *J Leukoc Biol* 83: 493-498, 2008.
32. **Haddad JJ.** On the enigma of pain and hyperalgesia: A molecular perspective. *Biochem Biophys Res Commun* 353: 217-224, 2007.
33. **Hardy KW and White TD.** Some commercial preparations of Escherichia coli bacterial endotoxin lipopolysaccharide (LPS) are contaminated with biologically active substances. *J Neurochem* 78: 1183-1184, 2001.
34. **Hausmann M, Kiessling S, Mestermann S, Webb G, Spottl T, Andus T, Scholmerich J, Herfarth H, Ray K, Falk W, and Rogler G.** Toll-like receptors 2 and 4 are up-regulated during intestinal inflammation. *Gastroenterology* 122: 1987-2000, 2002.
35. **Hayden MS and Ghosh S.** Shared principles in NF-kappaB signaling. *Cell* 132: 344-362, 2008.
36. **Hayden MS and Ghosh S.** Signaling to NF-kappaB. *Genes Dev* 18: 2195-2224, 2004.
37. **Hirschfeld M, Ma Y, Weis JH, Vogel SN, and Weis JJ.** Cutting edge: repurification of lipopolysaccharide eliminates signaling through both human and murine toll-like receptor 2. *J Immunol* 165: 618-622, 2000.

38. **Horwitz BJ and Fisher RS.** The irritable bowel syndrome. *N Engl J Med* 344: 1846-1850, 2001.
39. **Hou L and Wang X.** PKC and PKA, but not PKG mediate LPS-induced CGRP release and  $[Ca^{2+}]_i$  elevation in DRG neurons of neonatal rats. *J Neurosci Res* 66: 592-600, 2001.
40. **Hsu RY, Chan CH, Spicer JD, Rousseau MC, Giannias B, Rousseau S, and Ferri LE.** LPS-induced TLR4 signaling in human colorectal cancer cells increases beta1 integrin-mediated cell adhesion and liver metastasis. *Cancer Res* 71: 1989-1998, 2011.
41. <http://www.genemol.org/genemol/pictures/TRLsignaling.html>.
42. [http://www.prematueros.cl/weboctubre05/dolorfetal/dolor\\_fetal.html](http://www.prematueros.cl/weboctubre05/dolorfetal/dolor_fetal.html).
43. **Ibeakanma C, Miranda-Morales M, Richards M, Bautista-Cruz F, Martin N, Hurlbut D, and Vanner S.** *Citrobacter rodentium* colitis evokes post-infectious hyperexcitability of mouse nociceptive colonic dorsal root ganglion neurons. *J Physiol* 587: 3505-3521, 2009.
44. **Julius D and Basbaum AI.** Molecular mechanisms of nociception. *Nature* 413: 203-210, 2001.
45. **Kandel E, Schwartz J, and TM J.** *Principles of Neural Science*. New York, Unites States of America: McGraw-Hill, 2000.
46. **Kawai T and Akira S.** TLR signaling. *Semin Immunol* 19: 24-32, 2007.
47. **King DE, Macleod RJ, and Vanner SJ.** Trinitrobenzenesulphonic acid colitis alters Na<sub>v</sub>1.8 channel expression in mouse dorsal root ganglia neurons. *Neurogastroenterol Motil* 21: 880-e864, 2009.
48. **Kozuch PL and Hanauer SB.** Treatment of inflammatory bowel disease: a review of medical therapy. *World J Gastroenterol* 14: 354-377, 2008.
49. **Kraneveld AD, Rijniere A, Nijkamp FP, and Garssen J.** Neuro-immune interactions in inflammatory bowel disease and irritable bowel syndrome: future therapeutic targets. *Eur J Pharmacol* 585: 361-374, 2008.
50. **Kumar H, Kawai T, and Akira S.** Toll-like receptors and innate immunity. *Biochem Biophys Res Commun* 388: 621-625, 2009.
51. **Lakatos L.** Immunology of inflammatory bowel diseases. *Acta Physiol Hung* 87: 355-372, 2000.
52. **Lankiewicz S, Lobitz N, Wetzel CH, Rupprecht R, Gisselmann G, and Hatt H.** Molecular cloning, functional expression, and pharmacological

characterization of 5-hydroxytryptamine<sub>3</sub> receptor cDNA and its splice variants from guinea pig. *Mol Pharmacol* 53: 202-212, 1998.

53. **Lehnardt S, Massillon L, Follett P, Jensen FE, Ratan R, Rosenberg PA, Volpe JJ, and Vartanian T.** Activation of innate immunity in the CNS triggers neurodegeneration through a Toll-like receptor 4-dependent pathway. *Proc Natl Acad Sci U S A* 100: 8514-8519, 2003.

54. **Lewin GR, Lu Y, and Park TJ.** A plethora of painful molecules. *Curr Opin Neurobiol* 14: 443-449, 2004.

55. **Li X and Xu W.** TLR4-mediated activation of macrophages by the polysaccharide fraction from *Polyporus umbellatus*(pers.) Fries. *J Ethnopharmacol* 135: 1-6, 2011.

56. **Madden JA and Hunter JO.** A review of the role of the gut microflora in irritable bowel syndrome and the effects of probiotics. *Br J Nutr* 88 Suppl 1: S67-72, 2002.

57. **Malin S, Davis B, and Molliver D.** Production of dissociated sensory neuron cultures and considerations for their use in studying neuronal function and plasticity. *Nature Protocols* 2: 152-160, 2007.

58. **Marsh BJ and Stenzel-Poore MP.** Toll-like receptors: novel pharmacological targets for the treatment of neurological diseases. *Curr Opin Pharmacol* 8: 8-13, 2008.

59. **Medzhitov R.** Origin and physiological roles of inflammation. *Nature* 454: 428-435, 2008.

60. **Miller RJ, Jung H, Bhangoo SK, and White FA.** Cytokine and chemokine regulation of sensory neuron function. *Handb Exp Pharmacol*: 417-449, 2009.

61. **Miranda-Morales M, Ochoa-Cortes F, Stern E, Lomax AE, and Vanner S.** Axon reflexes evoked by transient receptor potential vanilloid 1 activation are mediated by tetrodotoxin-resistant voltage-gated Na<sup>+</sup> channels in intestinal afferent nerves. *J Pharmacol Exp Ther* 334: 566-575, 2010.

62. **North RA.** Molecular physiology of P2X receptors. *Physiol Rev* 82: 1013-1067, 2002.

63. **Ohland CL and Macnaughton WK.** Probiotic bacteria and intestinal epithelial barrier function. *Am J Physiol Gastrointest Liver Physiol* 298: G807-819, 2010.

64. **Ortega-Cava CF, Ishihara S, Rumi MA, Kawashima K, Ishimura N, Kazumori H, Udagawa J, Kadowaki Y, and Kinoshita Y.** Strategic

compartmentalization of Toll-like receptor 4 in the mouse gut. *J Immunol* 170: 3977-3985, 2003.

65. **Park SH, Kim ND, Jung JK, Lee CK, Han SB, and Kim Y.** Myeloid differentiation 2 as a therapeutic target of inflammatory disorders. *Pharmacol Ther* 133: 291-298, 2011.

66. **Perkins ND.** Integrating cell-signalling pathways with NF-kappaB and IKK function. *Nat Rev Mol Cell Biol* 8: 49-62, 2007.

67. **Raja S, Meyer R, Ringkamp M, and Campbell J.** Peripheral neural mechanisms of nociception. In: *Pain*, edited by Melzack R. London: Harcourt Publishers Ltd, 1999, p. 11-58.

68. **Sandoval E and Bosques-Padilla F.** Enfermedad inflamatoria intestinal: realidad en México. *Revista de Gastroenterología* 73: 38-42, 2008.

69. **Santos J, Guilarte M, Alonso C, and Malagelada JR.** Pathogenesis of irritable bowel syndrome: the mast cell connection. *Scand J Gastroenterol* 40: 129-140, 2005.

70. **Sartor RB.** Microbial influences in inflammatory bowel diseases. *Gastroenterology* 134: 577-594, 2008.

71. **Seksik P, Sokol H, Lepage P, Vasquez N, Manichanh C, Mangin I, Pochart P, Dore J, and Marteau P.** Review article: the role of bacteria in onset and perpetuation of inflammatory bowel disease. *Aliment Pharmacol Ther* 24 Suppl 3: 11-18, 2006.

72. **Shih DQ and Targan SR.** Immunopathogenesis of inflammatory bowel disease. *World J Gastroenterol* 14: 390-400, 2008.

73. **Simon AM, Veysiére G, and Jean C.** Structure and sequence of a mouse gene encoding an androgen-regulated protein: a new member of the seminal vesicle secretory protein family. *J Mol Endocrinol* 15: 305-316, 1995.

74. **Stewart T, Beyak MJ, and Vanner S.** Ileitis modulates potassium and sodium currents in guinea pig dorsal root ganglia sensory neurons. *J Physiol* 552: 797-807, 2003.

75. **Strober W, Fuss I, and Mannon P.** The fundamental basis of inflammatory bowel disease. *J Clin Invest* 117: 514-521, 2007.

76. **Wang B, Glatzle J, Mueller MH, Kreis M, Enck P, and Grundy D.** Lipopolysaccharide-induced changes in mesenteric afferent sensitivity of rat jejunum in vitro: role of prostaglandins. *Am J Physiol Gastrointest Liver Physiol* 289: G254-260, 2005.

77. **West AP, Koblansky AA, and Ghosh S.** Recognition and signaling by toll-like receptors. *Annu Rev Cell Dev Biol* 22: 409-437, 2006.

## X. APPENDIX B

**Ochoa-Cortes, F., Ramos-Lomas, T., Miranda-Morales, M., Ibeakanma, C, Barajas-Lopez, C., and Vanner, S.** Bacterial cell products signal to mouse colonic nociceptive ganglia neurons. *Am J Physiol Gastrointest Liver Physiol* 299: G723–G732, 2010.

## Bacterial cell products signal to mouse colonic nociceptive dorsal root ganglia neurons

Fernando Ochoa-Cortes,<sup>1,2</sup> Telma Ramos-Lomas,<sup>1,2</sup> Marcela Miranda-Morales,<sup>1,2</sup> Ian Spreadbury,<sup>1</sup> Charles Ibeakanma,<sup>1</sup> Carlos Barajas-Lopez,<sup>1,2</sup> and Stephen Vanner<sup>1</sup>

<sup>1</sup>Gastrointestinal Diseases Research Unit, Kingston General Hospital, Queen's University, Kingston, Ontario, Canada; and <sup>2</sup>Instituto Potosino de Investigacion Cientifica y Tecnologica, San Luis Potosi, Mexico

Submitted 8 December 2009; accepted in final form 17 June 2010

**Ochoa-Cortes F, Ramos-Lomas T, Miranda-Morales M, Spreadbury I, Ibeakanma C, Barajas-Lopez C, Vanner S.** Bacterial cell products signal to mouse colonic nociceptive dorsal root ganglia neurons. *Am J Physiol Gastrointest Liver Physiol* 299: G723–G732, 2010. First published June 24, 2010; doi:10.1152/ajpgi.00494.2009.—This study examined whether bacterial cell products that might gain access to the intestinal interstitium could activate mouse colonic nociceptive dorsal root ganglion (DRG) neurons using molecular and electrophysiological recording techniques. Colonic projecting neurons were identified by using the retrograde tracer fast blue and Toll-like receptor (TLR) 1, 2, 3, 4, 5, 6, 9, adapter proteins Md-1 and Md-2, and MYD88 mRNA expression was observed in laser-captured fast blue-labeled neurons. Ultrapure LPS 1  $\mu\text{g/ml}$  phosphorylated p65 NF- $\kappa\text{B}$  subunits increased transcript for TNF- $\alpha$  and IL-1 $\beta$  and stimulated secretion of TNF- $\alpha$  from acutely dissociated DRG neurons. In current-clamp recordings from colonic DRG neurons, chronic incubation (24 h) of ultrapure LPS significantly increased neuronal excitability. In acute studies, 3-min superfusion of standard-grade LPS (3–30  $\mu\text{g/ml}$ ) reduced the rheobase by up to 40% and doubled action potential discharge rate. The LPS effects were not significantly different in TLR4 knockout mice compared with wild-type mice. In contrast to standard-grade LPS, acute application of ultrapure LPS did not increase neuronal excitability in whole cell recordings or afferent nerve recordings from colonic mesenteric nerves. However, acute application of bacterial lysate (*Escherichia coli* NLM28) increased action potential discharge over 60% compared with control medium. Moreover, lysate also activated afferent discharge from colonic mesenteric nerves, and this was significantly increased in chronic dextran sulfate sodium salt mice. These data demonstrate that bacterial cell products can directly activate colonic DRG neurons leading to production of inflammatory cytokines by neurons and increased excitability. Standard-grade LPS may also have actions independent of TLR signaling.

LPS; NF- $\kappa\text{B}$ ; sensory neuronal excitability

THE INTESTINAL MICROBIOTA are increasingly recognized as important modulators of gastrointestinal (GI) function and may play a pivotal role in a number of GI disorders (9–11). Commensal bacteria signal to the innate immune system (2) and thereby alter the balance of pro- and anti-inflammatory cytokines. These actions may be particularly important in intestinal disorders such as inflammatory bowel disease and possibly irritable bowel syndrome (9, 22), in which increased epithelial permeability may allow bacteria access to the interstitial compartment of the intestine, thereby enhancing this signaling. Bacteria can also reach this interstitial compartment through the bloodstream, during generalized sepsis. Bacterial cell products have been shown in animal models to induce

hyperalgesia (6, 25, 31) and hence could contribute to sensory disturbances in these common human conditions. Understanding the pathways that underlie the ability of intestinal bacteria to alter sensory signaling in the intestine could potentially result in a new treatment paradigm for visceral pain.

Lipopolysaccharide (LPS), a component of the cell wall of gram-negative bacteria, has been shown to alter sensory pathways in the GI tract. In animal models, LPS has been shown to produce visceral hyperalgesia through an unknown mechanism. These studies demonstrate that LPS can stimulate discharge of mesenteric afferent nerves (26, 27, 33); however, it also resulted in local cytokine release following sustained luminal stimulation with LPS (19). Thus it is unclear whether LPS directly activates nociceptive neurons to induce altered sensory signaling or whether this occurs solely as a result of secondary effects of cytokine release.

Toll-like receptors (TLRs) play a key role in the innate recognition of microbial cell products such as LPS (20, 23, 24). These are type I transmembrane protein receptors that contain a leucine-rich repeat in the extracellular domain and a Toll/IL-1 repeat homology domain in the cytoplasmic region. At present, 10 TLRs have been identified in humans and 13 in mice (20). Genetic studies have shown these TLRs respond to a host of microbial products including LPS, nucleic acids, flagellin, peptidoglycan, and lipoproteins. All TLR signaling pathways lead to activation of the transcription factor NF- $\kappa\text{B}$  (19), which in turn controls the activation of inflammatory cytokine genes such as TNF- $\alpha$ , IL-1 $\beta$ , and IL-6. TLRs have been identified on multiple cell types in the GI tract (9, 20, 23), including intestinal epithelia cells and macrophages. Recent studies suggest TLR receptors may be found on neurons (29), but little is known about their expression on colonic nociceptive dorsal root ganglia (DRG) neurons.

To determine whether bacterial cell products can signal directly to nociceptive DRG neurons, we employed the retrograde marker fast blue dye to enable colonic DRG neurons to be identified. Using laser capture microdissection we demonstrated transcript of multiple TLRs in these neurons. We therefore employed molecular and perforated patch electrophysiological recording techniques to determine whether bacterial cell products activate these neurons.

### MATERIALS AND METHODS

Male CD1 and C57BL/6 mice (25–30 g) were obtained from Charles River Laboratories (Montreal, Quebec, Canada). C3H/HeJ TLR4 knockout and C3H/HeOuJ control background mice were obtained from The Jackson Laboratory (Bar Harbor, ME). Experiments were performed according to the guidelines of the Canadian

Address for reprint requests and other correspondence: S. Vanner, GI Diseases Research Unit, 76 Stuart St., Kingston General Hospital, Kingston, Ontario K7L 2V7, Canada (e-mail: vanners@hdh.kari.net).



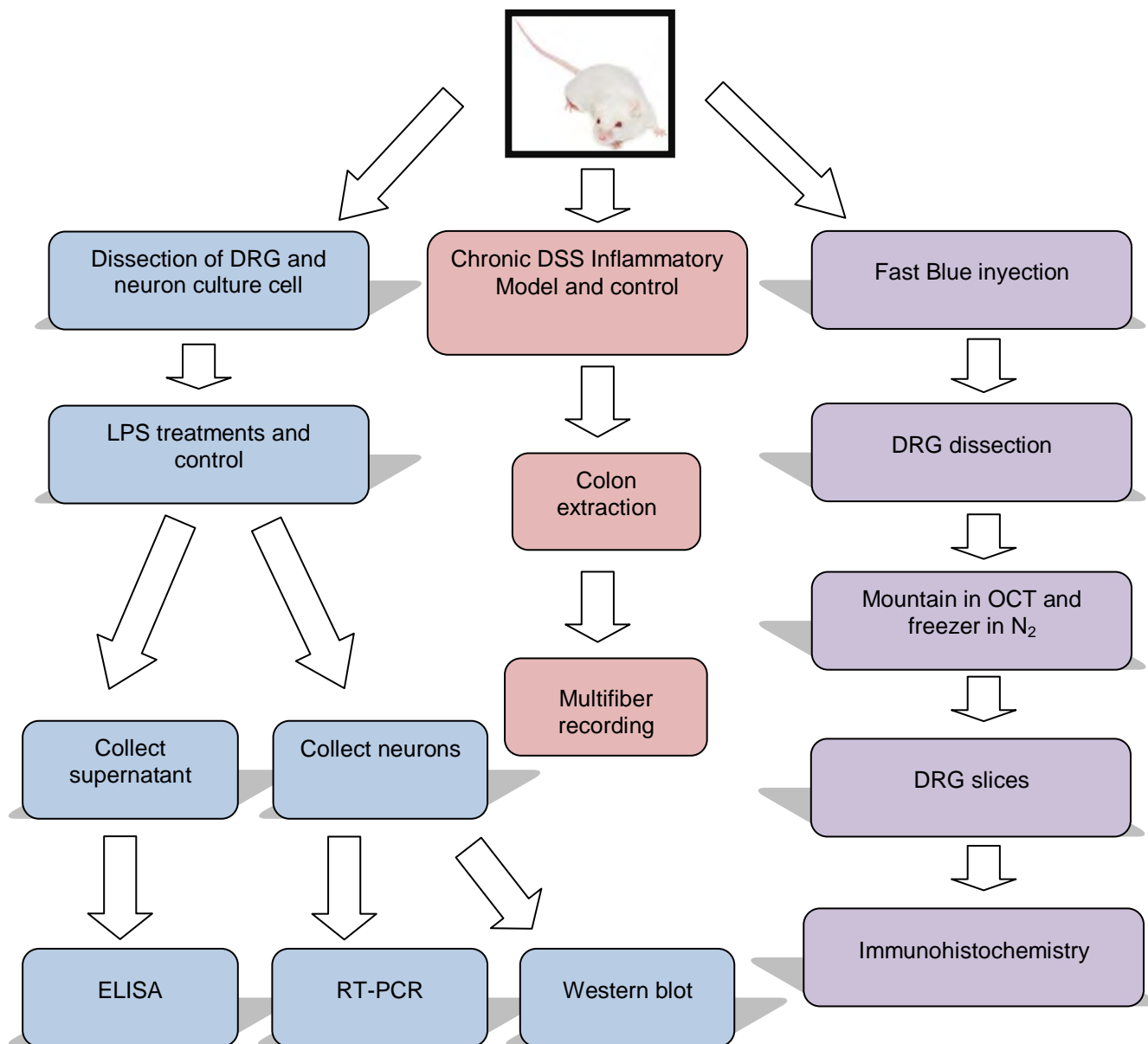


**Figure 10. Chart Flow of Experimental Protocols.**

### *Semiquantitative RT-PCR*

RT-PCR semiquantitative technique was used to determine the relative neuronal mRNAs levels for TNF- $\alpha$ , IL-6, IL-1 $\beta$ , NF $\kappa$ B and GAPDH. Total mRNA was obtained using Trizol Reagent (Invitrogen, Carlsbad, USA). cDNA was synthesized from 0.5  $\mu$ g total RNA with Oligo dT and SuperScript III (Invitrogen, Carlsbad, USA) for 50 min at 50°C. cDNA (0.5  $\mu$ l) was used as a template for PCR amplification in

## RESULTADOS

### *P2X5 de intestino de ratón*

En la figura A1 podemos observar que el P2X5 de ratón fue encontrado en el control positivo (cerebro) que fue utilizado. Las condiciones del PCR fueron: 55 °C de temperatura de alineamiento, utilizando *hot start* y 40 ciclos de amplificación. En el caso de P2X5 en intestino con esas mismas condiciones visualizamos una banda muy débil pero del tamaño esperado. Los productos de estos PCR fueron utilizados para la clonación en pGEM T-Easy y enviados a secuenciar.

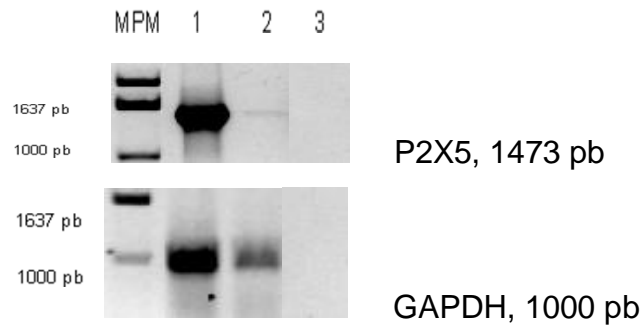


**Figura A1. P2X5 en intestino de ratón.** En la imagen superior observamos los productos de un PCR de 40 ciclos utilizando como templado cDNA de cerebro e intestino y en la inferior el de GAPDH como control. El marcador de peso molecular (MPM) utilizado fue 1 Kb de Invitrogen y los carriles corresponden a: 1- cerebro, 2- intestino y 3- control negativo. Los productos de PCR fueron corridos en geles de agarosa al 0.8% y fueron teñidos con bromuro de etidio.

Los plásmidos fueron enviados a secuenciar (McLab, California, E.U.) y dos de las secuencias dieron positivo para P2X5 con una similitud de 99%. Una de ellas retiene una secuencia de 267 pb (Figura A2.).

del 70%. El plásmido 2 pierde el exón 2, lo que introduce un codón de paro temprano a los 52 aa (Figura A3).

```

10      20      30      40      50      60      70      80      90
ggctgagctggcagcATGgggcaggcgggctggaagggcttctccagtcagcgttcgactataagacagaaaagtatgtgatcgccaag 90
aacaagaaggtcgggctgctctaccgactactgcagcttaccatcgtgctgtacctgatcgtatgggtgttcgtgataaagaagggttat 180
caagacactgacacctccctgcagagtgtgtggtcacaaagtcaagggcgtggcctacaccaacacctcagagctgggggagcgtctc 270
tgggacgtcgcagactacgtcatccccccaggagataatgtcttcttctgtgatcactaacctgatcgtgaccgccaaccagcggcag 360
agcacctgtgctgagcgtgaaggcattcctgatggcatgtgttctgaggaccacgactgccctgctggggagcctgttagagctggaat 450
ggagtgaagactggccgctgtctgcgggtggggaactcgaccaggggacacctgtgagatctttgcctgggtgccagtggaacacagtcc 540
aggccagggaagccactcctgagggagcgtgaagacttcaccatttccataaagaactataattcgtttcccaagtcaatttctccaag 630
gccaatgtactagagacaaagagcaagatatttctgaaatcctgtcgtttggccccaacaatcactatgtcccattctccggctgggg 720
tccgtggtccagtgggcagggagcagcttcaggacatgcccctggagggaggtgtgataggaattcacatcgagtggaactgcgacctc 810
gacagagctgcctctgagtgccatccgctctatttttaaccgtctggacgacaaacatgtaaaatctgttctctctgggtacaacttc 900
aggtttgccagataactaccgagactcagccgggtggaattccgcaacctgatgaaagcctatgggatccgcattgatgttatagttaat 990
ggaaaggcaggggaagttcagcatcgttcccacagtcacatcaatgtgggctccggggtggcgtcatgggtgctggggcttctctctgtgac 1080
ctggtactcatctacatcatcaaaaagagggagttttaccgtgacaaaagtacgaggaagtgaggggcccagagggggcggtcaggag 1170
gctgaggccaagggcgtggagcagggccagacggaggaggagcagcaggagggggagaggcaggaggagcagcctcagacctgccgag 1260
agcagcagctggaaggggaaacggcagcgtgtgcgggaagctgccccttcccagcaggaccagccttaaagcatgccaagggcgaatgta 1350
cagcaactgcagagctctgcagacagtgaggacgTAGccaaggctgtggccgagagcaggatttgaagatctgggccagcacagtctgc 1440
agctctgaactgggaagatgcatcctcatgcctgcgcga 1479

```

**Figura A4. Secuencia del cDNA del receptor P2X5.** El cDNA fue aislado de RNAm intestinal de quinea pig. El cDNA aislado tiene un longitud de 1479 bp. Las líneas naranjas indican la secuencia de los oligos y la letra mayúscula el comienzo del codón de inicio y de paro.

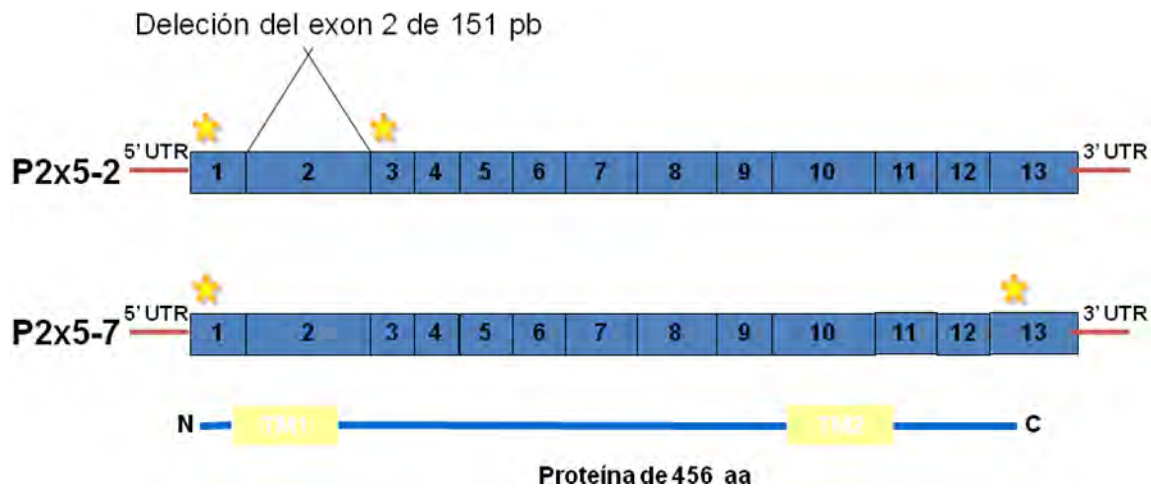


**Figura A5. Exones del P2X5 de cobayo.** La variante del plásmido 2 (que será conocida como variante 2) tiene deletado el exón 2 de 151 pb y la variante del plásmido 7 (que será conocida como variante 1) es la secuencia canónica de la subunidad P2X5 de intestino de cobayo que aún no ha sido reportada.

Las variantes se clonaron en el vector de expresión heteróloga pcDNA 3.1+ y se linearizaron para sintetizar el cRNA.